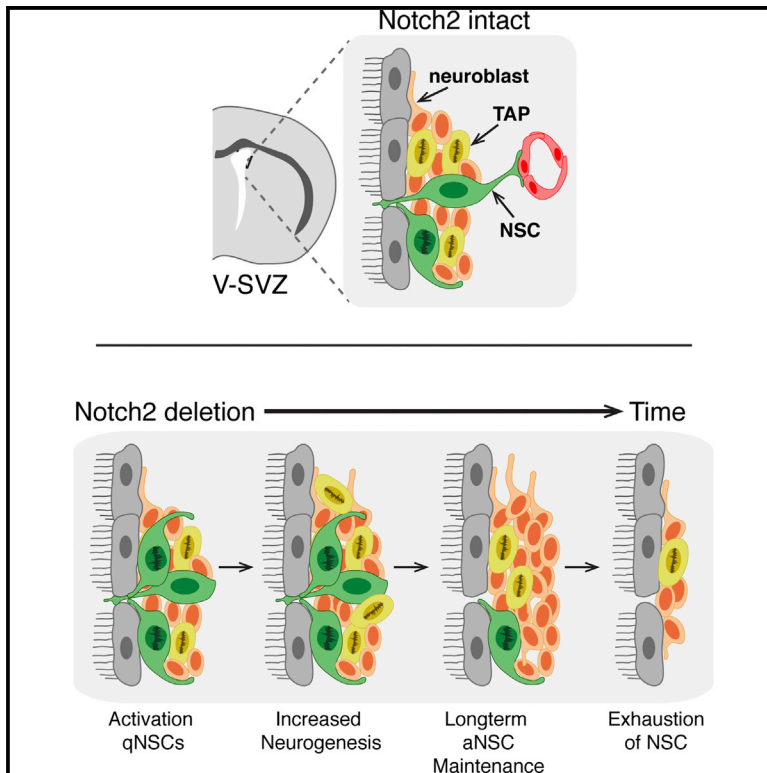


Notch2 Signaling Maintains NSC Quiescence in the Murine Ventricular-Subventricular Zone

Graphical Abstract



Authors

Anna Engler, Chiara Rolando, Claudio Giachino, ..., Spyros Artavanis-Tsakonas, Angeliki Louvi, Verdon Taylor

Correspondence

verdon.taylor@unibas.ch

In Brief

Using a combinatorial knockout approach, Engler et al. systematically analyze Notch signaling mutants. Their study demonstrates the role of Notch2 in the maintenance of quiescent NSCs in the adult murine brain.

Highlights

- Notch2 transduces a central quiescence signal in adult V-SVZ NSCs
- Loss of Notch2 leads to V-SVZ NSC activation and exhaustion
- Notch1 and Notch2 have distinct roles in NSC maintenance

Data and Software Availability

GSE99916



Notch2 Signaling Maintains NSC Quiescence in the Murine Ventricular-Subventricular Zone

Anna Engler,¹ Chiara Rolando,¹ Claudio Giachino,¹ Ichiko Saotome,² Andrea Erni,¹ Callum Brien,^{1,3} Runrui Zhang,¹ Ursula Zimmer-Strobl,⁴ Freddy Radtke,⁵ Spyros Artavanis-Tsakonas,⁶ Angeliki Louvi,² and Verdon Taylor^{1,7,*}

¹Department of Biomedicine, University of Basel, Mattenstrasse 28, 4058 Basel, Switzerland

²Departments of Neurosurgery and Neuroscience, Yale Program on Neurogenetics, Yale School of Medicine, New Haven, CT 06520, USA

³School of Science and Technology, Nottingham Trent University, Clifton Campus, NG11 8NS Nottingham, UK

⁴Department of Gene Vectors, Helmholtz Zentrum München, Marchioninistrasse 25, 81377 Munich, Germany

⁵EPFL SV ISREC UPAD, SV 2534 (Bâtiment SV), Station 19, 1015 Lausanne, Switzerland

⁶Department of Cell Biology, Harvard Medical School, Boston, MA 02115, USA

⁷Lead Contact

*Correspondence: verdon.taylor@unibas.ch

<https://doi.org/10.1016/j.celrep.2017.12.094>

SUMMARY

Neurogenesis continues in the ventricular-subventricular zone (V-SVZ) of the adult forebrain from quiescent neural stem cells (NSCs). V-SVZ NSCs are a reservoir for new olfactory bulb (OB) neurons that migrate through the rostral migratory stream (RMS). To generate neurons, V-SVZ NSCs need to activate and enter the cell cycle. The mechanisms underlying NSC transition from quiescence to activity are poorly understood. We show that Notch2, but not Notch1, signaling conveys quiescence to V-SVZ NSCs by repressing cell-cycle-related genes and neurogenesis. Loss of Notch2 activates quiescent NSCs, which proliferate and generate new neurons of the OB lineage. Notch2 deficiency results in accelerated V-SVZ NSC exhaustion and an aging-like phenotype. Simultaneous loss of Notch1 and Notch2 resembled the total loss of Rbpj-mediated canonical Notch signaling; thus, Notch2 functions are not compensated in NSCs, and Notch2 is indispensable for the maintenance of NSC quiescence in the adult V-SVZ.

INTRODUCTION

Somatic stem cells contribute to regeneration and repair in many adult tissues (Li and Clevers, 2010). They are embedded in specialized niches that control their maintenance, activation, and production of differentiated progeny (Cheung and Rando, 2013). Almost all tissues contain resident stem cells that rarely divide and are mitotically quiescent (Li and Clevers, 2010). Stem cell quiescence preserves the longevity of the progenitor pool, protects against the acquisition and propagation of genetic mutations, and counteracts hyperplasia and tumor formation (Adams et al., 2015; López-Otin et al., 2013). However, the mechanisms controlling quiescence and activation remain poorly understood (Cheung and Rando, 2013). Radial glia progenitors give rise to most neurons and glia of the mammalian neocortex during embryogenesis (Custo Greig et al., 2013; Fuentealba et al., 2015; Furutachi et al.,

2015; Malatesta et al., 2003; Merkle et al., 2007; Noctor et al., 2001; Rakic, 1972). Toward the end of embryonic development, neurogenesis ceases at most locations in the brain. Prime exceptions are the ventricular-subventricular zone (V-SVZ) of the lateral ventricle walls and the subgranular zone of the hippocampal dentate gyrus. In these distinct neurogenic niches, adult neural stem cells (NSCs) remain active and drive neurogenesis in rodents, non-human primates, and humans into adulthood (Doetsch, 2003; Doetsch et al., 1999; Ernst et al., 2014; Fuentealba et al., 2015; Furutachi et al., 2015; Spalding et al., 2013). In the V-SVZ, NSCs (also known as B1 cells) have a radial morphology, projecting bidirectionally through the ependymal lining of the striatal wall as well as to blood vessels underlying the V-SVZ (Fuentealba et al., 2012; Mirzadeh et al., 2008). B1 cells are quiescent and only sporadically enter the cell cycle to generate C cells, a mitotic population that amplifies the progenitor pool and gives rise to neuroblasts (A cells) (Fuentealba et al., 2012; Ihrie and Alvarez-Buylla, 2011). A cells migrate to the olfactory bulb (OB), where they differentiate into multiple interneuron subtypes that integrate into local circuits (Kirschenbaum et al., 1999; Lois et al., 1996).

Adult NSC maintenance and differentiation are tightly regulated by many factors, including Notch signaling (Andreu-Agulló et al., 2009; Basak et al., 2012; Ehm et al., 2010; Giachino et al., 2014; Imayoshi et al., 2010; Lugert et al., 2010; Nyfeler et al., 2005). Mammals have four Notch receptor paralogs, which signal in the same manner into the nucleus by forming a transcriptional activator complex that includes the canonical CSL transcription factor (CBF1 in humans, Suppressor of Hairless in *Drosophila*, Lag1 in *C. elegans* or Rbpj in mice). The Notch/CSL complex activates the expression of target genes, including *Hes* and *Hey* family members (Hatakeyama et al., 2004). *Hes5* is a functional readout of Notch signaling in NSCs, and *Hes5::GFP* or *Hes5::CreER^{T2}* transgenic alleles label NSCs and their progeny in the adult brain (Basak and Taylor, 2007; Giachino et al., 2014; Giachino and Taylor, 2009; Lugert et al., 2010, 2012). Deletion of *Rbpj* and inhibition of Notch signaling activate quiescent NSCs, block self-renewal, and result in a collapse of neurogenesis (Ehm et al., 2010; Imayoshi et al., 2010; Lugert et al., 2010). Interestingly, Notch1 regulates maintenance and self-renewal of active NSCs but is dispensable during quiescence, implying functional compensation by other Notch family



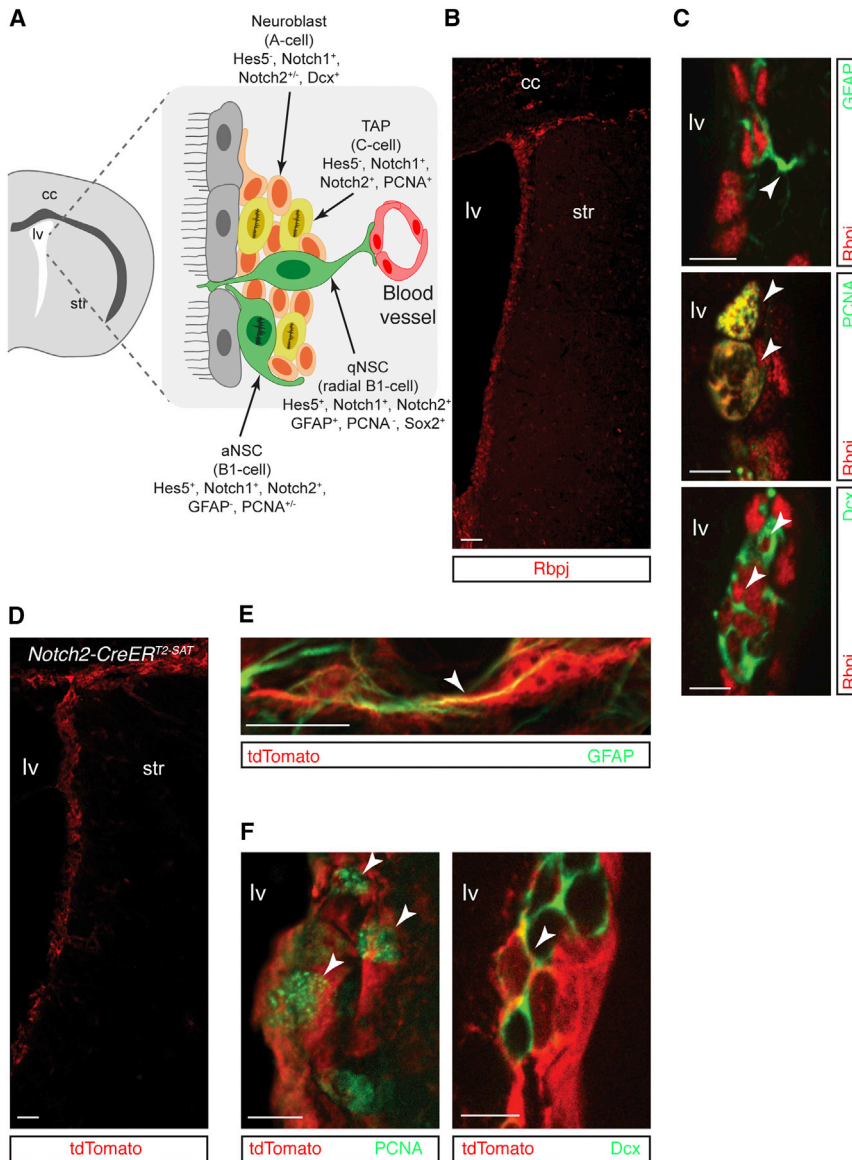


Figure 1. Notch Paralogues Are Broadly Expressed in the SVZ

(A) Hierarchical organization of adult neurogenesis in the V-SVZ. The V-SVZ is embedded between the lateral ventricle (lv), the corpus callosum (cc), and the striatum (str). Schematic view of the V-SVZ composition with cell-type-specific marker expression. ⁻, not expressed; ⁺, expressed; ^{+/+}, weak expression or expressed by few cells.

(B) Expression of *Rbpj* in the V-SVZ.

(C) Co-expression of *Rbpj* with glial fibrillary acid protein (GFAP), proliferating cell nuclear antigen (PCNA), or doublecortin (Dcx).

(D) Expression of tdTomato in *Notch2-CreER^{T2-SAT}* animals along the V-SVZ.

(E and F) Co-expression of tdTomato in *Notch2-CreER^{T2-SAT}* animals with GFAP (E) and with PCNA and Dcx (F; left and right, respectively). Notch signaling components are found ubiquitously throughout the V-SVZ and neurogenic lineage. Arrows point to *Rbpj* or tdTomato and marker double-positive cells.

Scale bars, 25 μ m in (B) and (C); 15 μ m in (D), (E), and (F) for GFAP and Dcx; and 10 μ m in (D) and (F) for PCNA.

See also Figure S1 and Table S1.

(Giachino et al., 2014; Imayoshi et al., 2010). Conditional deletion of *Rbpj* or *Notch1* from NSCs of the V-SVZ resulted in overlapping yet partially distinct phenotypes (Basak et al., 2012; Imayoshi et al., 2010). Whereas *Rbpj* cKO resulted in activation of NSCs, a transient increase in neurogenesis, and precocious exhaustion of the entire pool, *Notch1* cKO decreased neurogenesis and the active NSC pool but did not activate quiescent NSCs (Basak et al., 2012; Imayoshi et al., 2010).

We examined the expression of *Rbpj* and *Notch2* in the V-SVZ compared to the expression reported for *Notch1*

(Basak et al., 2012). Here, we address how Notch signaling regulates NSC quiescence by combinatorial conditional knockout (cKO) of *Notch1*, *Notch2*, and *Rbpj* genes. We deleted *Notch1*, *Notch2*, and *Rbpj* from *Hes5::CreER^{T2}*-expressing NSCs in the V-SVZ of adult mice and analyzed the effects, comparing and contrasting the phenotypes. Our findings revealed that *Notch2* regulates adult NSC quiescence and that combinatorial cKO of *Notch1* and *Notch2* phenocopies a total loss of canonical Notch signaling induced by *Rbpj* cKO.

RESULTS

Notch Signaling Components Are Ubiquitously Expressed in the Neurogenic Lineage

Quiescent and activated V-SVZ NSCs express the Notch target gene *Hes5*, indicating canonical Notch signaling

(Basak et al., 2012; Nyfeler et al., 2005). As expected from the genetic data, *Rbpj* is broadly expressed in the V-SVZ, including GFAP⁺ putative NSCs, as well as 100% of the actively dividing progenitors (transient amplifying progenitors [TAPs]; PCNA⁺) and Dcx⁺ neuroblasts (Figures 1A–1C, S1A, and S1B; Table S1). To identify *Notch2*-expressing cells in the adult mouse V-SVZ, we performed tamoxifen-induced, short-term lineage tracing in *Notch2-CreER^{T2}* animals using a *Rosa26R::tdTomato* Cre-reporter allele (Figure S1C) (Fre et al., 2011). The majority of the GFAP⁺ B1-like putative NSCs and mitotic TAPs (PCNA⁺) were labeled with tdTomato (93.8% \pm 5.9% and 93.8% \pm 2.8%, respectively), as were Dcx⁺ neuroblasts (42.4% \pm 12.7%). This indicates that *Notch2* is expressed broadly by cells of the neurogenic lineage in the V-SVZ, confirming our previous observations (Figures 1D–1F, S1D, and S1E; Table S1) (Basak et al., 2012). Some Dcx⁺ neuroblasts were genetically labeled

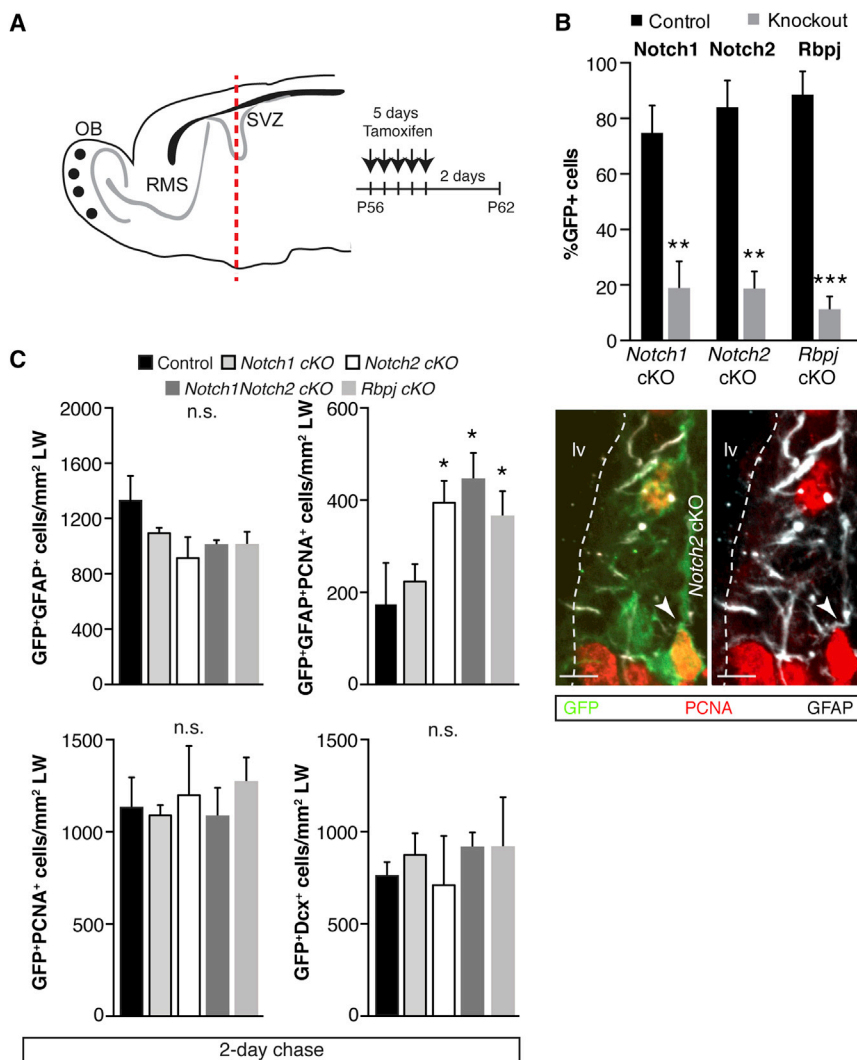


Figure 2. Acute Loss of Notch Signaling Results in Activation of quiescent NSCs

(A) Schematic representation of the adult mouse brain. Brains were analyzed on coronal sections at the level of the red bar after 5 days of tamoxifen administration and a short 2-day chase period.

(B) Quantification of recombination efficiency in knockout animals. Protein levels of recombined alleles were significantly reduced.

(C) Quantification of *Hes5::CreER^{T2}*-derived (GFP+) GFP+GFAP+, GFP+GFAP+PCNA+ NSCs (B1 cells), GFP+PCNA+ proliferating progenitors, or GFP+Dcx+ neuroblasts in the V-SVZ of control, *Notch1* cKO, *Notch2* cKO, *Notch1Notch2* cKO, and *Rbpj* cKO mice 2 days post-tamoxifen induction. GFP+GFAP+PCNA+ mitotic radial NSCs (B1 cells) in the V-SVZ in *Notch2* cKO mice (arrow-head).

Values are means \pm SD. * $p < 0.05$; ** $p < 0.01$; *** $p < 0.001$. n.s., not significant. 2-day chase: control $n = 5$; *Notch1* cKO $n = 6$; *Notch2* cKO $n = 5$; *Notch1Notch2* cKO $n = 4$; and *Rbpj* cKO $n = 4$. Scale bars, 10 μ m in (C).

See also Figure S2 and Tables S2 and S3.

the GFP+ labeled cells. Recombination was restricted to GFAP+ NSCs, including proliferating PCNA+Dcx- B1 cells. TAPs and Dcx+ neuroblasts were not labeled, confirming restriction of *Hes5::CreER^{T2}* expression to NSCs (Figure S1G) (Lugert et al., 2012).

Shortly after the induction of gene deletion (2-day chase), *Rbpj*, *Notch1*, and *Notch2* cKO mutants all displayed a similar level of genetic labeling and a 75%–85% reduction in the proportion of targeted V-SVZ cells that expressed the respective proteins encoded by the targeted genes (Figures 2A, 2B, S2A, and S2B; Table S2A).

Deletion of *Rbpj*, *Notch1Notch2*, or *Notch2* resulted in the rapid activation of normally quiescent GFP+GFAP+ NSCs and their entry into the cell cycle (GFP+GFAP+PCNA+; Figure 2C). In contrast, *Notch1* cKO did not result in the activation of quiescent NSCs, confirming previous observations (Basak et al., 2012). At 2 days, the increased proliferation of NSCs did not affect the total number of GFP+ cells in the V-SVZ of any of the mutants, and the total number of GFP+GFAP+ stem cells, proliferating TAPs (GFAP+GFP+PCNA+), or GFP+Dcx+ neuroblasts was not changed (Figure 2C; Tables S2B and S2C). Therefore, *Notch2* cKO, but not *Notch1* cKO, mirrored the activation of quiescent NSCs observed following *Rbpj* or *Notch1Notch2* cKO. This suggested that Notch2 signaling conveys quiescence to V-SVZ NSCs.

To examine the effects of the loss of Notch2 and provide insights into how it may regulate NSC activity, we isolated *Notch2* cKO cells from the V-SVZ 1 day after ablation and performed genome-wide gene expression analysis (Figures S2C–S2G; Tables S2 and S3). Notch2 mRNA levels were significantly

(tdTomato+) after short-term tracing of tamoxifen-induced *Notch2-CreER^{T2}* animals and likely represents the expression of Notch2 by some newborn neuroblasts and nascent production of neuroblasts from Notch2-expressing progenitors during the labeling period and chase.

To address whether the activation of quiescent NSCs following loss of *Rbpj*, but not loss of Notch1, was the result of Notch-independent functions of *Rbpj* or molecular compensation of Notch1 and Notch2 in V-SVZ NSCs, we conditionally deleted *Rbpj^{flox/flox}*, *Notch1^{flox/flox}*, *Notch2^{flox/flox}*, or, simultaneously, *Notch1^{flox/flox}* and *Notch2^{flox/flox}* alleles from *Hes5::CreER^{T2}*-expressing NSCs, and followed their fate and progeny using a *Rosa26R::GFP* Cre-reporter (Figure S1F) (Besseyrias et al., 2007; Han et al., 2002; Lugert et al., 2012; Radtke et al., 1999; Schouwwey et al., 2007; Tchorz et al., 2012). In order to confirm the cellular specificity of *Hes5::CreER^{T2}* expression in the V-SVZ, we performed a low-dose tamoxifen induction followed by a short-term chase in *Hes5::CreER^{T2}* *Rosa26R::GFP* animals (controls) and analyzed lineage-marker expression by

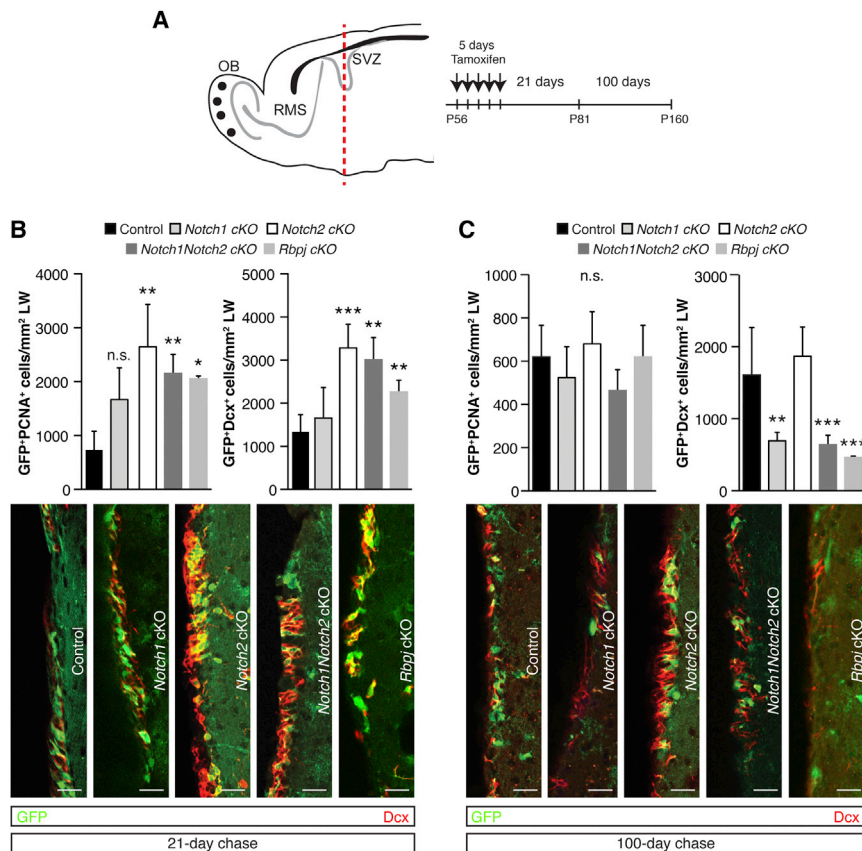


Figure 3. Notch1 and Notch2 Have Distinct Functions in Adult Neurogenesis

(A) Schematic representation of the mouse brain. Brains were analyzed on coronal sections at the level of the red bar after 5 days of tamoxifen administration and 21-day or 100-day chase period in control, *Notch1* cKO, *Notch2* cKO, *Notch1Notch2* cKO, or *Rbpj* cKO animals. (B) Quantification and analysis of *Hes5::CreERT2*-derived (GFP⁺) progeny in the V-SVZ of control, *Notch1* cKO, *Notch2* cKO, *Notch1Notch2* cKO, and *Rbpj* cKO mice 21 days post-tamoxifen induction. GFP⁺PCNA⁺ proliferating cells and GFP⁺Dcx⁺ neuroblasts were increased in *Notch2* cKO, *Notch1Notch2* cKO, and *Rbpj* cKO animals. Images are of GFP⁺Dcx⁺ neuroblasts in the V-SVZ control versus mutant animals. (C) Quantification of GFP⁺PCNA⁺ proliferating cells showed no significant change at 100 days, whereas GFP⁺Dcx⁺ neuroblasts in the V-SVZ were decreased in *Notch1* cKO, *Notch1Notch2* cKO, and *Rbpj* cKO mice 100 days post-tamoxifen induction. Images are of GFP⁺Dcx⁺ neuroblasts in the V-SVZ control versus mutant animals. Values are means \pm SD. * $p < 0.05$; ** $p < 0.01$; *** $p < 0.001$. n.s., not significant. 21-day chase: control $n = 6$; *Notch1* cKO $n = 4$; *Notch2* cKO $n = 5$; *Notch1Notch2* cKO $n = 6$; and *Rbpj* cKO $n = 4$. 100-day chase: control $n = 5$; *Notch1* cKO $n = 4$; *Notch2* cKO $n = 4$; *Notch1Notch2* cKO $n = 4$; and *Rbpj* cKO $n = 4$. Scale bars, 25 μ m. See also Figure S3 and Table S4.

decreased, confirming gene ablation, and hierarchical gene clustering revealed significant differences in gene expression between *Notch2* cKO and control cells ($R^2 = 0.8289$; 2,126 mRNAs 2-fold, 469 mRNAs 4-fold, and 71 mRNAs 8-fold changed; Figures S2D and S2E; Table S3). Within the top gene ontology categories for differentially expressed genes, there were neurogenesis ($p = 3.92 \times 10^{-28}$), neurological processes ($p = 2.64 \times 10^{-18}$), Notch signaling pathway ($p = 9.21 \times 10^{-15}$), and cell cycle ($p = 1.47 \times 10^{-8}$) (Figure S2F). In agreement with the phenotype observed in the V-SVZ of the *Notch2* cKO mice, genes associated with stem cell maintenance ($p = 1.46 \times 10^{-6}$) were also affected by the *Notch2* cKO. Loss of Notch2 led to rapid changes in the transcriptome, particularly in genes involved in neuron differentiation ($p = 2.21 \times 10^{-13}$) and OB interneuron differentiation ($p = 4.2 \times 10^{-11}$). Furthermore, genes linked to gliogenesis ($p = 1.2 \times 10^{-5}$), glia cell differentiation ($p = 7.8 \times 10^{-3}$), and oligodendrocytes ($p = 0.023$) were also significantly changed after *Notch2* cKO (Figure S2G). Thus, the gene expression analysis confirmed that *Notch2* cKO affected genes associated with NSC proliferation and differentiation.

Notch1 cKO and Notch2 cKO Reveal Non-redundant Functions in the V-SVZ

In order to address the role of Notch2 in NSC activation and differentiation of their progeny within the lineage, we examined the consequences of loss of Notch signaling components in

the V-SVZ at distinct time points and along the rostral migratory stream (RMS) to the OB. To compare the long-term effects of Notch paralog and *Rbpj* deletion, we analyzed cKO mice 21 days and 100 days after gene deletion (Figure 3A). 21 days after deletion, the overall number of GFP⁺ cells in the V-SVZ was significantly increased in *Notch2* cKO, *Notch1Notch2* cKO, and *Rbpj* cKO animals, compared with controls (Figure S3A; Table S4A). The increase in the number of proliferating TAPs (GFP⁺PCNA⁺) and neuroblasts (GFP⁺Dcx⁺) in these animals contributed to the increase in GFP⁺ cells (Figure 3B; Table S4B). Conversely, the number of GFP⁺GFAP⁺ NSCs was not changed in any of the mutants (Figures S3B and S3C; Table S4B). While both the total number and the fraction of proliferating GFP⁺GFAP⁺PCNA⁺ NSCs were reduced in the *Rbpj* and *Notch2* cKO animals, proliferative TAPs (GFP⁺PCNA⁺) and neuroblasts (GFP⁺Dcx⁺PCNA⁺) were increased (Figures S3B–S3D; Table S4B). It is tempting to speculate that a negative-feedback loop from the NSC progeny inhibits the proliferation of the remaining NSCs (GFP⁺GFAP⁺) and that this is enhanced in the *Rbpj* and *Notch2* cKO animals due to the increase in TAPs and neuroblasts (Aguirre et al., 2010; Rolando et al., 2012). A similar repressive feedback from the progeny to the NSCs may also explain the observed increase in proliferation of GFP⁺GFAP⁺ cells in *Notch1* cKO animals (Figures S3B and S3C; Table S4B). These results support the hypothesis that Notch2

regulates maintenance of quiescent NSCs, whereas Notch1 is critical for the maintenance of neurogenic NSCs.

In order to address the long-term effects of *Notch2* deletion, we examined animals 100 days after tamoxifen administration. 100 days after gene deletion, the number of GFP⁺ cells in the V-SVZ of *Notch2* cKO animals had returned to the levels observed in control animals but were significantly reduced in *Notch1Notch2* cKO and *Rbpj* cKO animals (Figure S3E; Table S4A). This was in line with the observation that none of the mutants showed increased levels of proliferation at this stage. Additionally, all mutants, with the exception of the *Notch2* cKO animals, showed a significant reduction in GFP⁺Dcx⁺ neuroblasts. The *Notch1* cKO with the *Hes5::CreER^{T2}* reported here is consistent with previous data showing loss of neuroblasts in the V-SVZ following cKO with a *Nestin::CreER^{T2}* allele (Basak et al., 2012). The levels of GFP⁺Dcx⁺ in the *Notch2* cKO mutants also reduced between the 21-day ($3,284.5 \pm 342.3$) and 100-day ($1,897.7 \pm 327.9$) chases, albeit to a lesser extent than in *Notch1Notch2* cKO (21-day chase: $3,008.5 \pm 328.9$ versus 100-day chase: 550.5 ± 73.4) and *Rbpj* cKO mutants (21-day chase: $2,426.3 \pm 147.4$ versus 100-day chase: 461.7 ± 8.5). Thus, *Notch2* cKO animals showed a unique phenotype after a 100-day chase that was not observed in *Notch1* cKO, *Notch1Notch2* cKO, or *Rbpj* cKO animals (Figure 3C; Table S4C). The persistence of neuroblasts in the *Notch2* cKO animals is in line with the observation that the overall GFP⁺ cell number in *Notch2* cKO mutants was not different from that in controls at this stage, despite the initial increase observed at 21 days.

The numbers of GFP⁺GFAP⁺ and GFP⁺GFAP⁺PCNA⁺ NSCs were reduced in *Notch2* cKO, *Notch1Notch2* cKO, and *Rbpj* cKO animals, again implicating a crucial role of Notch2 in quiescent NSC maintenance. This hypothesis is underlined by the observation that only *Notch2* cKO animals, 100 days after deletion, retain an increased number of newly produced GFP⁺Dcx⁺PCNA⁺ neuroblasts. These changes were observed both at the number of cells per square millimeter (Figure S3F; Table S4C) and at the population level (Figure S3G; Table S4C).

NSC Activation Increases Neuroblast Generation down the RMS and into the OB

Notch2 cKO animals are phenotypically distinct from the *Notch1*, *Notch1Notch2*, or *Rbpj* cKO animals within the V-SVZ. We addressed the effects of Notch receptor signaling on OB neurogenesis. The effects of *Rbpj* cKO on OB neurogenesis have been described previously, and as *Notch1Notch2* cKO phenocopied these effects, we focused on the *Notch1* cKO, *Notch2* cKO, and *Notch1Notch2* cKO animals in the further analysis (Imayoshi et al., 2010). We traced neuroblasts migrating in the RMS toward the OB in control animals and *Notch1* cKO, *Notch2* cKO, and *Notch1Notch2* cKO mutants 21 and 100 days after tamoxifen treatment (Figure 4A; Table S5A). After a 21-day chase, GFP⁺Dcx⁺ neuroblasts in the RMS were significantly increased in the *Notch2* and *Notch1Notch2* cKO mutants, compared with controls and *Notch1* cKO animals. This also resulted in an increase in the cross-sectional area of the RMS (Figures 4B and S4A; Table S5A). Thus, the increase in neurogenesis in the V-SVZ projects into the RMS of *Notch2* and *Notch1Notch2* cKO animals 21 days after gene deletion. After a 100-day chase, GFP⁺ cells and GFP⁺Dcx⁺ neuroblasts were reduced in the RMS

of *Notch1* cKO, *Notch2* cKO, and *Notch1Notch2* cKO animals, compared with controls. The cross-sectional area of the RMS in *Notch1* cKO and *Notch2* cKO animals was indistinguishable from that in controls but significantly reduced in *Notch1Notch2* cKO animals (Figure 4C; Table S5B).

Neuroblasts from the RMS migrated to the OB and distributed to the granule cell layer (GCL) and the glomeruli. 21 days after tamoxifen induction, the first *Hes5::CreER^{T2}* NSC-derived neuroblasts had migrated through the RMS and started to radiate to the OB layers (Figures 5A and 5B). *Notch2* and *Notch1Notch2* cKO mutants showed an increase in neuroblasts (GFP⁺Dcx⁺) in the GCL (Figure 5C; Table S6A). This increase in newly generated granule cells was due to the global increase in neuroblasts and not improper fate commitment in *Notch2* and *Notch1Notch2* cKO animals (Figure S5A). *Notch1Notch2* cKO animals showed an increase in GFP⁺NeuN⁺ neurons, indicating a more rapid onset of terminal differentiation compared with control, *Notch1* cKO, or *Notch2* cKO animals (Figure S5B; Table S6A). At this time point, newly formed neurons had not reached the glomeruli (Figure S5C; Table S6A).

After 100 days, the number of neuroblasts (GFP⁺Dcx⁺) in the GCL remained increased in the *Notch2* cKO and *Notch1Notch2* cKO animals, indicating a prolonged enhancement of neurogenesis, but we did not find evidence of a cell-fate switch (Figures 5D, 5E, and S5D; Table S6B). However, *Notch1Notch2* cKO animals still displayed an increase in newly generated GFP⁺NeuN⁺ mature neurons in the GCL (Figures 5E and S5E; Table S6B). The overall number of GFP⁺ cells per square millimeter of the GCL in the *Notch2* cKO and *Notch1Notch2* cKO animals was almost double that in controls, supporting the hypothesis that neurogenesis was increased, whereas *Notch1* cKO animals showed a reduced number of GFP⁺ cells in the OB (Figure S5F; Table S6B). 100 days after gene deletion, new neurons had also reached the glomeruli, and the number of GFP⁺NeuN⁺ neurons and the total number of GFP⁺ cells were increased in the *Notch2* cKO and *Notch1Notch2* cKO animals, but not *Notch1* cKO animals, compared to those in controls (Figure S5G; Table S6C). These results indicate that loss of Notch2 signaling causes precocious differentiation and neurogenesis in the V-SVZ, resulting in more neurons in the OB.

Loss of Notch Signaling Results in NSC Depletion and Loss of Neurogenesis

The age-related decline in adult neurogenesis has been linked, at least in part, to NSC exhaustion. As *Notch2* cKO animals showed an increase in neurogenesis following a 100-day chase, we asked whether *Notch2* cKO animals were able to maintain this increased neuron production for a long period of time or whether they exhibited precocious progenitor exhaustion. We analyzed the Notch mutant animals after 300 days. The overall number of GFP⁺ cells in the V-SVZ was reduced in *Notch1* cKO, *Notch2* cKO, and *Notch1Notch2* cKO mutants (Figure 6A; Table S7A). Similarly, the numbers of GFP⁺GFAP⁺ NSCs, newborn proliferating GFP⁺PCNA⁺ cells (TAPs), and GFP⁺Dcx⁺ neuroblasts were also reduced in the Notch mutant animals, compared to those of controls (Figures 6A, 6B, and S6A; Tables S7A and S7B).

The reduction in NSCs, TAPs, and neuroblasts in the V-SVZ resulted in a significant reduction in GFP⁺Dcx⁺ neuroblasts in the OB GCL of the mutant animals after a 300-day chase

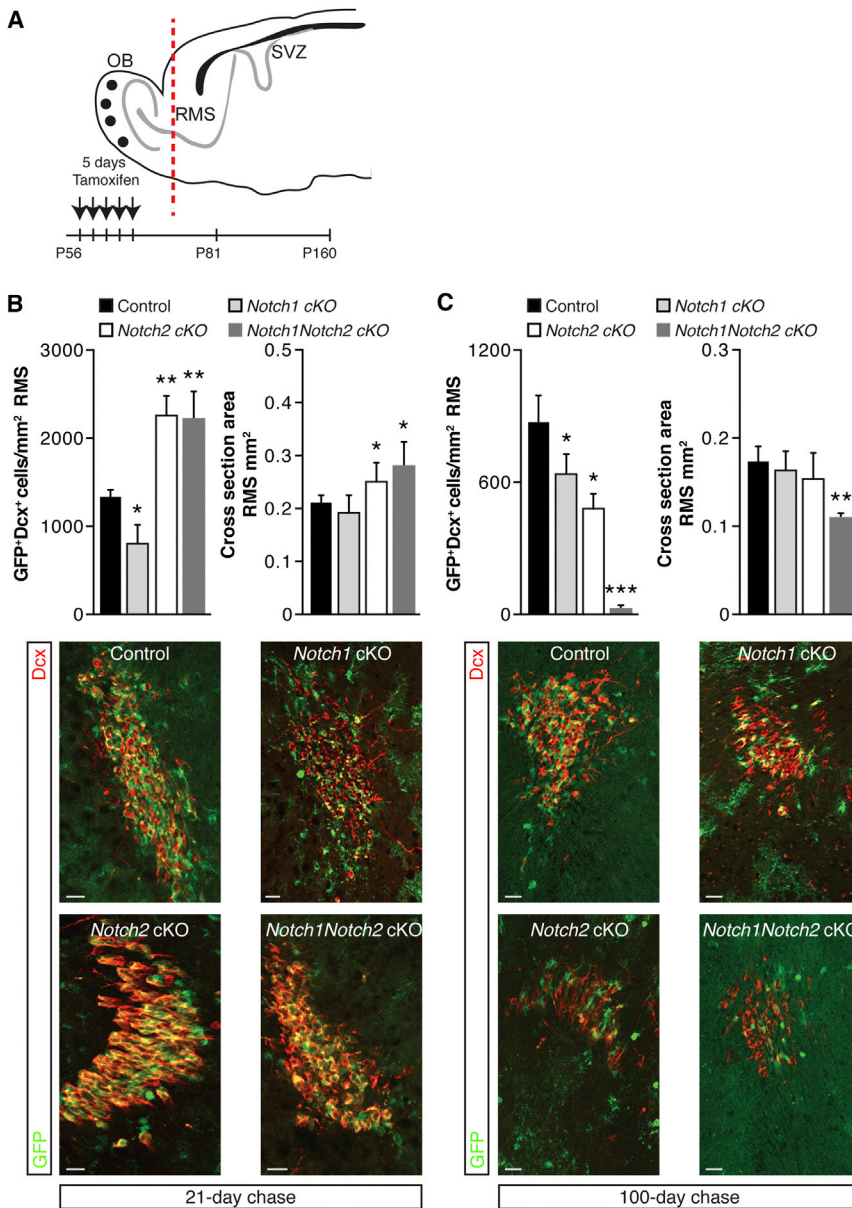


Figure 4. NSC Activation Projects down the RMS

(A) Schematic representation of the mouse brain. Brains were analyzed on coronal sections at the level of the red bar after 5 days of tamoxifen administration and 21-day or 100-day chase period in control, *Notch1* cKO, *Notch2* cKO, or *Notch1Notch2* cKO animals.

(B) Quantification and analysis of *Hes5::CreERT2*-derived (GFP⁺) progeny in the RMS 21 days post-tamoxifen induction. Images are of GFP⁺Dcx⁺ neuroblasts in the RMS of control, *Notch2* cKO, and *Notch1Notch2* cKO animals.

(C) Quantification and analysis of NSC progeny in the RMS 100 days post-tamoxifen induction. Values are means \pm SD. * $p < 0.05$; ** $p < 0.01$; *** $p < 0.001$. n.s., not significant. 21-day chase: control $n = 6$; *Notch2* cKO $n = 5$; and *Notch1Notch2* cKO $n = 6$. 100-day chase: control $n = 5$; *Notch2* cKO $n = 4$; and *Notch1Notch2* cKO $n = 4$. Scale bars, 25 μ m. See also Figure S4 and Table S5.

animals at 100 days (Figure S3G), were slightly reduced at 300 days (Figure S6A), suggesting a more gradual NSC depletion during aging after *Notch1* loss, similar to our previous observations (Basak et al., 2012).

In summary, we show that *Notch2* regulates the activation of otherwise quiescent NSCs and that loss of *Notch2* culminates in precocious neurogenesis in the V-SVZ and a wave of increased neuron formation in the OB (Figures 7 and S7). In contrast, loss of *Notch1* results in the differentiation and exhaustion of activated NSCs. Our comparative analysis of mutant mice indicates that *Notch* signaling in the V-SVZ OB system controls the early steps of neurogenesis but does not affect the differentiation fate and neuronal subtype generated in the adult OB. Our results indicate that *Notch1* and *Notch2* play distinct roles in V-SVZ neuro-

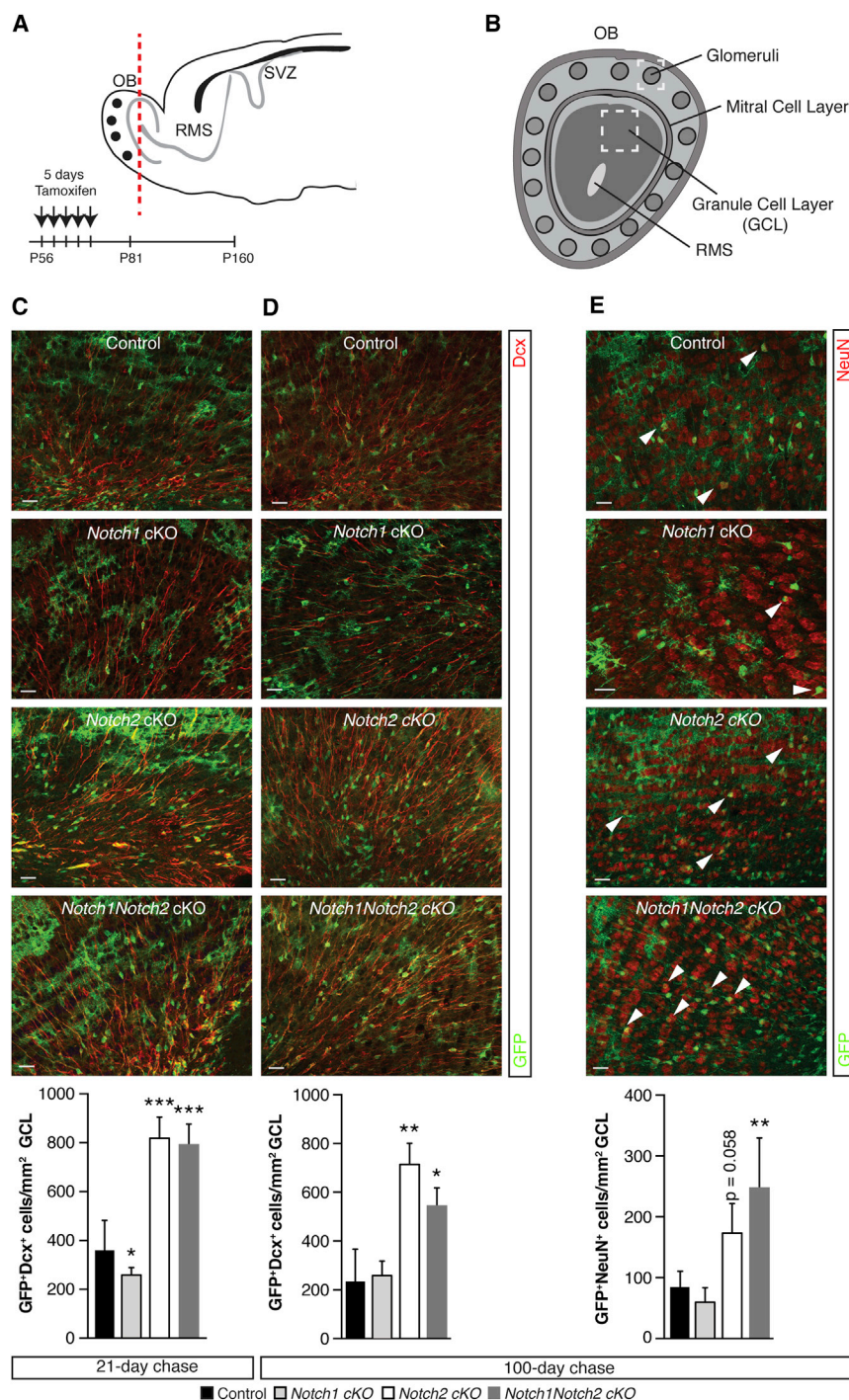
genesis and that *Notch2* is a key regulator of NSC quiescence and maintenance. The fact that loss of *Notch2* and activation of the quiescent NSC pool result in a rapid decline in neurogenesis and a premature aging phenotype in the V-SVZ implies that the quiescent pool is, indeed, a reservoir for new neurons in the adult brain (Figure 7). The parallels between loss of *Notch2* and *Rbpj* in the decline in NSC number indicate that *Notch2* regulation of NSC quiescence through *Rbpj* is critical for V-SVZ homeostasis.

(Figure 6C; Table S7C). Furthermore, the number of GFP⁺NeuN⁺ neurons in the *Notch2* cKO and *Notch1Notch2* cKO animals was similar to that of controls, whereas *Notch1* cKO animals contained slightly reduced numbers of GFP⁺NeuN⁺ neurons (Figure 6C; Table S7C). In line with this, the total number of GFP⁺ cells in the GCL and the glomeruli was comparable to that of controls in the *Notch2* cKO and *Notch1Notch2* cKO animals (Figures S6B and S6C; Table S7D). These results indicate that NSCs in the *Notch2* cKO and *Notch1Notch2* cKO animals are depleted and that the neurogenic capacity of the V-SVZ is reduced. Hence, the initial increase in neuron production in the *Notch2* cKO and *Notch1Notch2* cKO animals is followed over time by a loss of NSCs and a decline in progenitors in the V-SVZ. GFAP⁺ NSCs, which were initially not changed in *Notch1* cKO

animals at 100 days (Figure S3G), were slightly reduced at 300 days (Figure S6A), suggesting a more gradual NSC depletion during aging after *Notch1* loss, similar to our previous observations (Basak et al., 2012).

DISCUSSION

The control of stem cell activity and their entry into the cell cycle is critical for tissue homeostasis, regeneration, and protection



against tumor formation by guarding against propagation of genetic mutations (Doetsch, 2003). In the adult V-SVZ, most NSCs are mitotically inactive. Quiescent NSCs enter the cell cycle infrequently to generate active NSCs that produce newborn neurons that migrate to the OB (Lois et al., 1996). Genetic loss-of-function experiments in mice indicated that Rbpj and Notch1 are important regulators of V-SVZ neurogenesis; however, their phenotypes exhibit clear differences, particularly in the activa-

tion of the quiescent NSC pool. Whereas loss of Rbpj induces quiescent NSCs to enter the cell cycle, Notch1 deletion does not (Basak et al., 2012; Imayoshi et al., 2010). These differences could reflect molecular compensation of Notch1 by other Notch family members, the different experimental paradigms used, different Rbpj and Notch1 protein stabilities, or Notch-independent roles of Rbpj. To distinguish between these possibilities, we generated mice with conditional deletions of *Rbpj*, *Notch1*, *Notch2*, or *Notch1* and *Notch2* using the same *Hes5::CreER^{T2}* driver and undertook a detailed analysis of neurogenesis in the V-SVZ of these Notch signaling cKO adult animals.

First, and importantly, we demonstrated that simultaneous deletion of *Notch1* and *Notch2* phenocopied the deletion of *Rbpj* (Imayoshi et al., 2010). Therefore, the observed effects of delet-

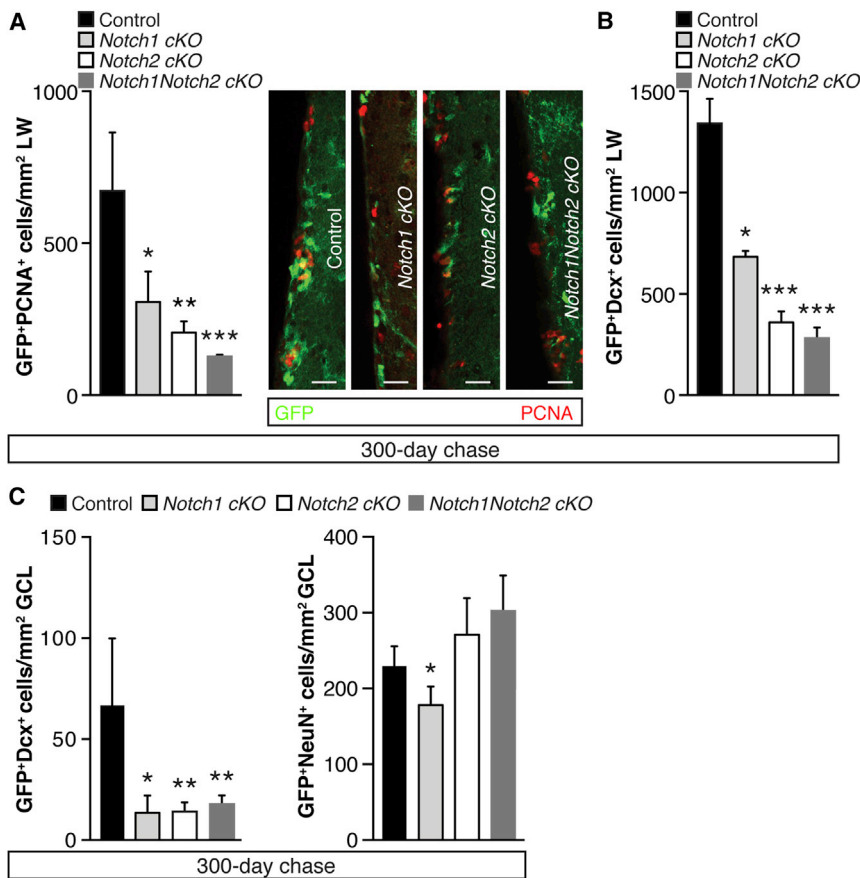


Figure 6. Long-Term Ablation of Notch Signaling Results in NSC Loss and Depletion of Neurogenesis

(A and B) Shown here: (A) quantification and imaging of proliferating GFP+PCNA+ cells and (B) quantification of GFP+Dcx+ cells in the V-SVZ in control, *Notch1* cKO, *Notch2* cKO, and *Notch1Notch2* cKO mice 300 days post-tamoxifen administration.

(C) Quantification of GFP+Dcx+ neuroblasts and GFP+NeuN+ neurons in the GCL 300 days after tamoxifen administration in control, *Notch1* cKO, *Notch2* cKO, and *Notch1Notch2* cKO animals. Values are means \pm SD. * $p < 0.05$; ** $p < 0.01$; *** $p < 0.001$. 300-day chase: control $n = 4$; *Notch2* cKO $n = 3$; and *Notch1Notch2* cKO $n = 3$. Scale bars, 25 μ m.

See also Figure S6 and Table S7.

How Notch signaling can play different roles in different cells or in the same cell in different states has remained a major question. Our finding that Notch2 can repress V-SVZ NSC activation while Notch1 maintains active neurogenic NSCs, presumably during asymmetric cell division, is intriguing, as it implies that the coexpression of Notch1 and Notch2 is not merely a pre-emptive, compensatory mechanism but that both receptors play necessary roles in V-SVZ neurogenesis. The interplay between

NSCs and their niche is highlighted after Notch1 deletion. Initially, and in contrast to mice in which *Notch2* or *Rbpj* had been deleted, *Notch1* cKO did not result in an immediate activation of quiescent NSCs. However, 21 days later, and once neurogenesis had declined in the *Notch1* cKO, the quiescent radial NSCs activated and entered the cell cycle, presumably to compensate for the loss of neuroblasts and active neurogenic population. These findings support the hypothesis that the quiescent NSC pool is a reserve that can feed into the lineage once the active neurogenic cells become exhausted or are lost (Aguirre et al., 2010).

Deletion of *Rbpj* from astrocytes within the mouse striatum has been reported to initiate neuronal production, lending support for our finding that Notch2 prevents both entry into the cell cycle and the generation of neurons from V-SVZ NSCs (Magnusson et al., 2014). However, the loss of Notch receptors using the *Hes5::CreER^{T2}* allele, which also targets some astrocytes in the brain parenchyma including the striatum, did not induce ectopic neurogenesis or proliferation, even 300 days after cKO. These differences could be due to the targeting of different astrocyte subpopulations in the two experiments but indicates that deletion of *Rbpj* and Notch receptors does not automatically lead to neuron production by astrocytes in the brain, supporting the notion that the local niche and cell potential play critical roles in neurogenesis.

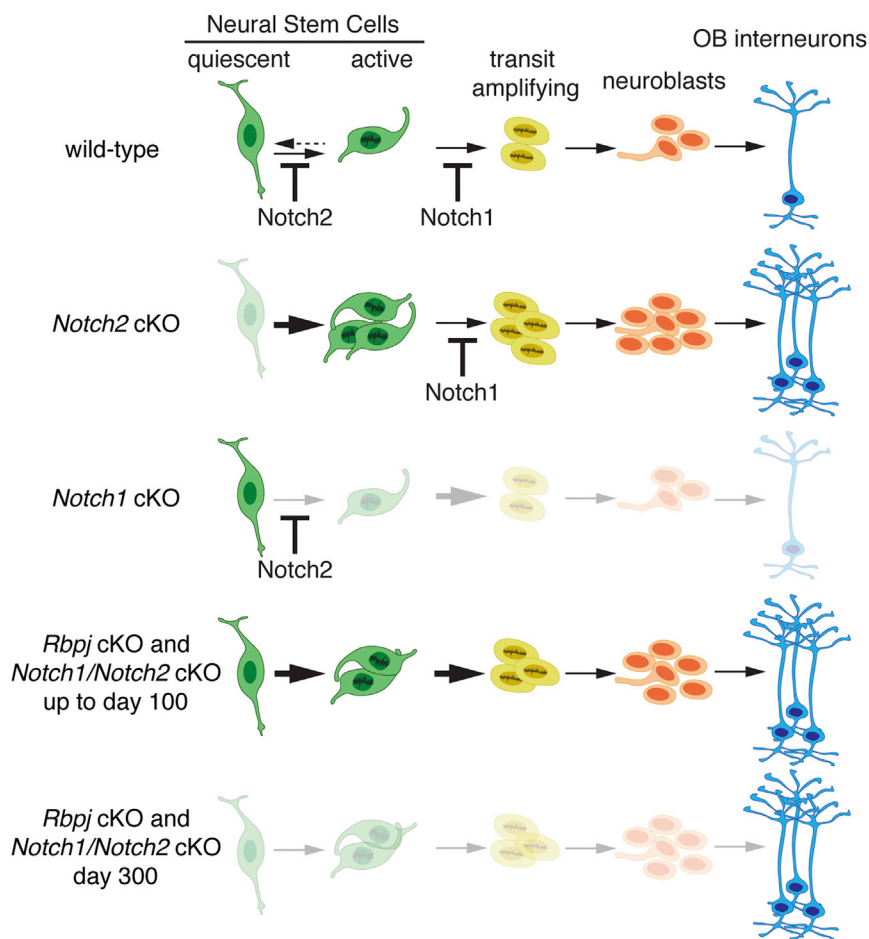


Figure 7. Notch Ablation Affects the Neurogenic Lineage

Summary of the changes within the lineage of the neurogenic adult V-SVZ of *Notch1* cKO, *Notch2* cKO, *Notch1Notch2* cKO, and *Rbpj* cKO animals at day 100 post-gene ablation compared to control animals, showing increases and decreases in the specific cell types. The proposed actions of blocking the lineage progression of Notch1 and Notch2 are shown. For the *Notch1Notch2* cKO and *Rbpj* cKO animals, the effects of gene ablation are shown for time periods up to day 100 and at day 300 after gene ablation. See also Figure S7.

lethal dose of ketamine-xylazine and perfused transcardially. Tissue was cut into sections 30 μ m thick (Supplemental Experimental Procedures) (Giachino and Taylor, 2009; Lugert et al., 2010).

Microarray Analysis and qRT-PCR

Animals were sacrificed 24 hr after tamoxifen treatment. Tissue was prepared for fluorescence-activated cell sorting (FACS), as described previously (Lugert et al., 2010), and GFP⁺ cells were sorted directly in TRIzol reagent (Thermo Fisher Scientific). RNA was extracted according to manufacturer's recommendations. RNA quality was tested by Fragment Analyzer (Advanced Analytical). cDNA was prepared using BioScript (Bioline). qRT-PCR was performed using the SensiMix SYBR kit (Bioline). Affymetrix expression profiling was performed on Affymetrix GeneChip Mouse Gene 1.0 ST arrays (ATLAS Biolabs). Gene ontology (GO) analysis was performed using Lasergene ArrayStar (DNASTAR). The microarray data are available at GEO: GSE99916. For detailed information, see the Supplemental Experimental Procedures and Table S3.

Quantification and Statistical Analysis

Stained sections were analyzed with a Zeiss Observer with Apotome (Zeiss). Images were processed with Photoshop or ImageJ. Data are presented as averages of a minimum of three sections per region and multiple animals (n in the figure legends). Statistical significance was determined by two-tailed Student's t test on mean values per animal, and percentages were transformed into their arcsin values. Significance was determined as *p < 0.05, **p < 0.01, and ***p < 0.001; or p values are given in the graphs. Deviance from the mean is displayed as SD, if not otherwise indicated. Complete data tables are provided in the Supplemental Information.

DATA AND SOFTWARE AVAILABILITY

The accession number for the microarray datasets reported in this paper is GEO: GSE99916.

SUPPLEMENTAL INFORMATION

Supplemental Information includes Supplemental Experimental Procedures, seven figures, and seven tables and can be found with this article online at <https://doi.org/10.1016/j.celrep.2017.12.094>.

In summary, we show that Notch2 regulates adult neurogenesis in the V-SVZ by preserving NSC quiescence. By direct and comparable genetic ablation experiments, we found that, although coexpressed by the same cells in the V-SVZ, different Notch receptors play distinct roles in regulating NSC activity and fate. How Notch1 and Notch2 specifically control different aspects of adult neurogenesis remains to be shown.

EXPERIMENTAL PROCEDURES

Animals and Husbandry

Hes5::GFP, *Hes5::CreER^{T2}*, *Notch2::CreER^{T2-SAT}*, *Rosa26R::GFP*, *Rosa26R::tdTomato*, floxed *Notch1*, floxed *Notch2*, and floxed *Rbpj* mice have been described elsewhere (Basak et al., 2012; Basak and Taylor, 2007; Besseyrias et al., 2007; Fre et al., 2011; Lugert et al., 2012; Schouwey et al., 2007). Experiments were conducted as gender unbiased, with a minimum of three animals per experimental group. Mice were kept according to Swiss Federal and Swiss Veterinary office regulations under license numbers 2537 and 2538 (Ethics commission Basel-Stadt, Basel Switzerland). For further information see the Supplemental Experimental Procedures.

Administration of Tamoxifen and Tissue Preparation

Adult mice 8–10 weeks of age were injected daily intraperitoneally with 2 mg tamoxifen in corn oil for 5 consecutive days and killed 2, 21, 100, or 300 days after the end of the treatment. Animals were given a

ACKNOWLEDGMENTS

We thank the members of the Taylor lab for critical reading of the manuscript and for helpful discussions and Frank Sager for excellent technical assistance. We thank Dr. H.R. MacDonald for the Notch2 antibodies and Dr. T. Honjo for floxed *Rbpj* mice. We thank the animal core facility of the University of Basel and the BioOptics Facility of the Department of Biomedicine for support. This work was supported by the Swiss National Science Foundation (310030_143767 to V.T.), covering salaries and consumables; the University of Basel, covering salaries, consumables, overheads, and animal costs; the Forschungsfonds University of Basel (to A. Engler), covering salary; and Bio-gen (to A.L.), covering salary, animal costs, and consumables.

AUTHOR CONTRIBUTIONS

Conceptualization, V.T., A. Engler, C.R., and C.G.; Investigation, A. Engler, C.R., A. Erni, I.S., C.B., and R.Z.; Writing – Original Draft, A. Engler and V.T.; Writing – Review and Editing, A. Engler, V.T., C.R., C.G., A. Erni, C.B., and R.Z.; Funding Acquisition, V.T., A.L., and A.E.; Project Administration, V.T.; Resources, A.L., S.A.-T., U.Z.-S., F.R., and V.T.

DECLARATION OF INTERESTS

The authors declare no competing interests.

Received: August 25, 2016

Revised: June 12, 2017

Accepted: December 22, 2017

Published: January 23, 2018

REFERENCES

- Adams, P.D., Jasper, H., and Rudolph, K.L. (2015). Aging-induced stem cell mutations as drivers for disease and cancer. *Cell Stem Cell* 16, 601–612.
- Aguirre, A., Rubio, M.E., and Gallo, V. (2010). Notch and EGFR pathway interaction regulates neural stem cell number and self-renewal. *Nature* 467, 323–327.
- Andreu-Agulló, C., Morante-Redolat, J.M., Delgado, A.C., and Fariñas, I. (2009). Vascular niche factor PEDF modulates Notch-dependent stemness in the adult subependymal zone. *Nat. Neurosci.* 12, 1514–1523.
- Basak, O., and Taylor, V. (2007). Identification of self-replicating multipotent progenitors in the embryonic nervous system by high Notch activity and *Hes5* expression. *Eur. J. Neurosci.* 25, 1006–1022.
- Basak, O., Giachino, C., Fiorini, E., Macdonald, H.R., and Taylor, V. (2012). Neurogenic subventricular zone stem/progenitor cells are Notch1-dependent in their active but not quiescent state. *J. Neurosci.* 32, 5654–5666.
- Besseyrias, V., Fiorini, E., Strobl, L.J., Zimmer-Strobl, U., Dumortier, A., Koch, U., Arcangeli, M.L., Ezine, S., Macdonald, H.R., and Radtke, F. (2007). Hierarchy of Notch-Delta interactions promoting T cell lineage commitment and maturation. *J. Exp. Med.* 204, 331–343.
- Chapouton, P., Skupien, P., Hesl, B., Coolen, M., Moore, J.C., Madeline, R., Kremmer, E., Faus-Kessler, T., Blader, P., Lawson, N.D., and Bally-Cuif, L. (2010). Notch activity levels control the balance between quiescence and recruitment of adult neural stem cells. *J. Neurosci.* 30, 7961–7974.
- Cheung, T.H., and Rando, T.A. (2013). Molecular regulation of stem cell quiescence. *Nat. Rev. Mol. Cell Biol.* 14, 329–340.
- Custo Greig, L.F., Woodworth, M.B., Galazo, M.J., Padmanabhan, H., and Macklis, J.D. (2013). Molecular logic of neocortical projection neuron specification, development and diversity. *Nat. Rev. Neurosci.* 14, 755–769.
- Doetsch, F. (2003). The glial identity of neural stem cells. *Nat. Neurosci.* 6, 1127–1134.
- Doetsch, F., Caillé, I., Lim, D.A., García-Verdugo, J.M., and Alvarez-Buylla, A. (1999). Subventricular zone astrocytes are neural stem cells in the adult mammalian brain. *Cell* 97, 703–716.

- Ehm, O., Göritz, C., Covic, M., Schäffner, I., Schwarz, T.J., Karaca, E., Kempkes, B., Kremmer, E., Pfriger, F.W., Espinosa, L., et al. (2010). RBPJkappa-dependent signaling is essential for long-term maintenance of neural stem cells in the adult hippocampus. *J. Neurosci.* 30, 13794–13807.
- Ernst, A., Alkass, K., Bernard, S., Salehpour, M., Perl, S., Tisdale, J., Possnert, G., Druid, H., and Frisén, J. (2014). Neurogenesis in the striatum of the adult human brain. *Cell* 156, 1072–1083.
- Fre, S., Hannezo, E., Sale, S., Huyghe, M., Lafkas, D., Kissel, H., Louvi, A., Greve, J., Louvard, D., and Artavanis-Tsakonas, S. (2011). Notch lineages and activity in intestinal stem cells determined by a new set of knock-in mice. *PLoS ONE* 6, e25785.
- Fuentealba, L.C., Obernier, K., and Alvarez-Buylla, A. (2012). Adult neural stem cells bridge their niche. *Cell Stem Cell* 10, 698–708.
- Fuentealba, L.C., Rompani, S.B., Parraguez, J.L., Obernier, K., Romero, R., Cepko, C.L., and Alvarez-Buylla, A. (2015). Embryonic origin of postnatal neural stem cells. *Cell* 161, 1644–1655.
- Furutachi, S., Miya, H., Watanabe, T., Kawai, H., Yamasaki, N., Harada, Y., Imayoshi, I., Nelson, M., Nakayama, K.I., Hirabayashi, Y., and Gotoh, Y. (2015). Slowly dividing neural progenitors are an embryonic origin of adult neural stem cells. *Nat. Neurosci.* 18, 657–665.
- Giachino, C., and Taylor, V. (2009). Lineage analysis of quiescent regenerative stem cells in the adult brain by genetic labelling reveals spatially restricted neurogenic niches in the olfactory bulb. *Eur. J. Neurosci.* 30, 9–24.
- Giachino, C., Basak, O., Lugert, S., Knuckles, P., Obernier, K., Fiorelli, R., Frank, S., Raineteau, O., Alvarez-Buylla, A., and Taylor, V. (2014). Molecular diversity subdivides the adult forebrain neural stem cell population. *Stem Cells* 32, 70–84.
- Han, H., Tanigaki, K., Yamamoto, N., Kuroda, K., Yoshimoto, M., Nakahata, T., Ikuta, K., and Honjo, T. (2002). Inducible gene knockout of transcription factor recombination signal binding protein-J reveals its essential role in T versus B lineage decision. *Int. Immunol.* 14, 637–645.
- Hatakeyama, J., Bessho, Y., Katoh, K., Ookawara, S., Fujioka, M., Guillemot, F., and Kageyama, R. (2004). *Hes* genes regulate size, shape and histogenesis of the nervous system by control of the timing of neural stem cell differentiation. *Development* 131, 5539–5550.
- Ihrle, R.A., and Alvarez-Buylla, A. (2011). Lake-front property: a unique germinal niche by the lateral ventricles of the adult brain. *Neuron* 70, 674–686.
- Imayoshi, I., Sakamoto, M., Yamaguchi, M., Mori, K., and Kageyama, R. (2010). Essential roles of Notch signaling in maintenance of neural stem cells in developing and adult brains. *J. Neurosci.* 30, 3489–3498.
- Kawai, H., Kawaguchi, D., Kuebrich, B.D., Kitamoto, T., Yamaguchi, M., Gotoh, Y., and Furutachi, S. (2017). Area-specific regulation of quiescent neural stem cells by Notch3 in the adult mouse subependymal zone. *J. Neurosci.* 37, 11867–11880.
- Kirschenbaum, B., Doetsch, F., Lois, C., and Alvarez-Buylla, A. (1999). Adult subventricular zone neuronal precursors continue to proliferate and migrate in the absence of the olfactory bulb. *J. Neurosci.* 19, 2171–2180.
- Li, L., and Clevers, H. (2010). Coexistence of quiescent and active adult stem cells in mammals. *Science* 327, 542–545.
- Lois, C., García-Verdugo, J.M., and Alvarez-Buylla, A. (1996). Chain migration of neuronal precursors. *Science* 271, 978–981.
- López-Otín, C., Blasco, M.A., Partridge, L., Serrano, M., and Kroemer, G. (2013). The hallmarks of aging. *Cell* 153, 1194–1217.
- Lugert, S., Basak, O., Knuckles, P., Haussler, U., Fabel, K., Götz, M., Haas, C.A., Kempermann, G., Taylor, V., and Giachino, C. (2010). Quiescent and active hippocampal neural stem cells with distinct morphologies respond selectively to physiological and pathological stimuli and aging. *Cell Stem Cell* 6, 445–456.
- Lugert, S., Vogt, M., Tchorz, J.S., Müller, M., Giachino, C., and Taylor, V. (2012). Homeostatic neurogenesis in the adult hippocampus does not involve amplification of *Ascl1*(high) intermediate progenitors. *Nat. Commun.* 3, 670.

- Magnusson, J.P., Göritz, C., Tatarishvili, J., Dias, D.O., Smith, E.M., Lindvall, O., Kokaia, Z., and Frisén, J. (2014). A latent neurogenic program in astrocytes regulated by Notch signaling in the mouse. *Science* **346**, 237–241.
- Malatesta, P., Hack, M.A., Hartfuss, E., Kettenmann, H., Klinkert, W., Kirchhoff, F., and Götz, M. (2003). Neuronal or glial progeny: regional differences in radial glia fate. *Neuron* **37**, 751–764.
- Merkle, F.T., Mirzadeh, Z., and Alvarez-Buylla, A. (2007). Mosaic organization of neural stem cells in the adult brain. *Science* **317**, 381–384.
- Mirzadeh, Z., Merkle, F.T., Soriano-Navarro, M., Garcia-Verdugo, J.M., and Alvarez-Buylla, A. (2008). Neural stem cells confer unique pinwheel architecture to the ventricular surface in neurogenic regions of the adult brain. *Cell Stem Cell* **3**, 265–278.
- Noctor, S.C., Flint, A.C., Weissman, T.A., Dammerman, R.S., and Kriegstein, A.R. (2001). Neurons derived from radial glial cells establish radial units in neocortex. *Nature* **409**, 714–720.
- Nyfeler, Y., Kirch, R.D., Mantei, N., Leone, D.P., Radtke, F., Suter, U., and Taylor, V. (2005). Jagged1 signals in the postnatal subventricular zone are required for neural stem cell self-renewal. *EMBO J.* **24**, 3504–3515.
- Radtke, F., Wilson, A., Stark, G., Bauer, M., van Meerwijk, J., MacDonald, H.R., and Aguet, M. (1999). Deficient T cell fate specification in mice with an induced inactivation of Notch1. *Immunity* **10**, 547–558.
- Rakic, P. (1972). Mode of cell migration to the superficial layers of fetal monkey neocortex. *J. Comp. Neurol.* **145**, 61–83.
- Rolando, C., Parolisi, R., Boda, E., Schwab, M.E., Rossi, F., and Buffo, A. (2012). Distinct roles of Nogo-a and Nogo receptor 1 in the homeostatic regulation of adult neural stem cell function and neuroblast migration. *J. Neurosci.* **32**, 17788–17799.
- Schouwey, K., Delmas, V., Larue, L., Zimmer-Strobl, U., Strobl, L.J., Radtke, F., and Beermann, F. (2007). Notch1 and Notch2 receptors influence progressive hair graying in a dose-dependent manner. *Dev. Dyn.* **236**, 282–289.
- Spalding, K.L., Bergmann, O., Alkass, K., Bernard, S., Salehpour, M., Huttner, H.B., Boström, E., Westerlund, I., Vial, C., Buchholz, B.A., et al. (2013). Dynamics of hippocampal neurogenesis in adult humans. *Cell* **153**, 1219–1227.
- Tchorz, J.S., Suply, T., Ksiazek, I., Giachino, C., Cloëta, D., Danzer, C.P., Doll, T., Isken, A., Lemaistre, M., Taylor, V., et al. (2012). A modified RMCE-compatible Rosa26 locus for the expression of transgenes from exogenous promoters. *PLoS ONE* **7**, e30011.

Supplemental Information

Notch2 Signaling Maintains NSC Quiescence in the Murine Ventricular-Subventricular Zone

Anna Engler, Chiara Rolando, Claudio Giachino, Ichiko Saotome, Andrea Erni, Callum Brien, Runrui Zhang, Ursula Zimmer-Strobl, Freddy Radtke, Spyros Artavanis-Tsakonas, Angeliki Louvi, and Verdon Taylor

SUPPLEMENTAL DATA AND INFORMATION

SUPPLEMENTAL FIGURES AND LEGENDS

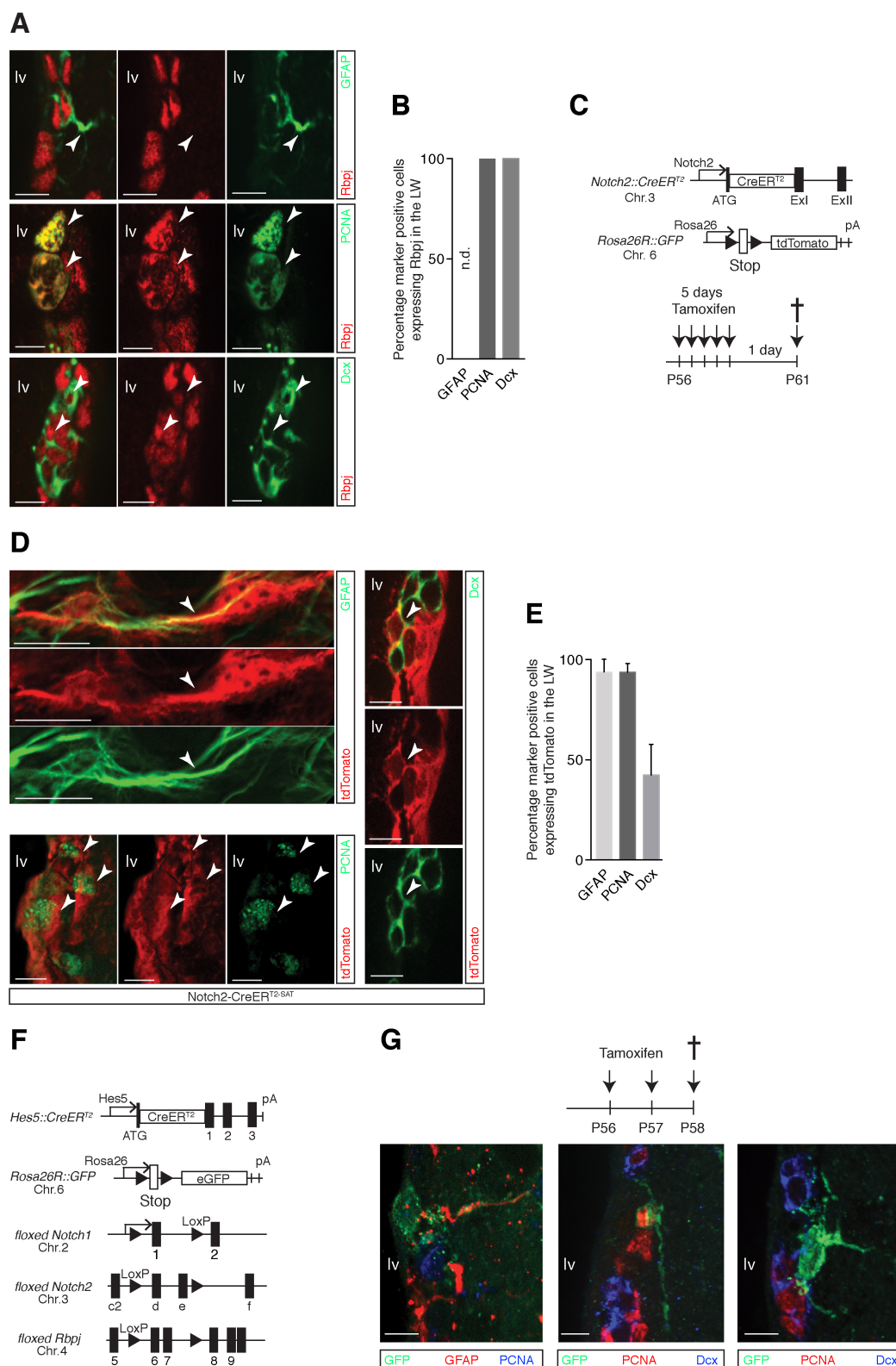


Figure S1. Notch paralogues are broadly expressed in the V-SVZ. Related to Figure 1 and Table S1.

A. Expression of *Rbpj* with GFAP, PCNA or Dcx showing individual color channels of Figure 1C. Arrows point to *Rbpj* and marker double-positive cells. **B.** Quantification of coexpression of GFAP, PCNA or Dcx with *Rbpj*. n.d. – not determined. **C.** Schematic representation of *Notch2-CreER^{T2-SAT}* transgene and *Rosa26R::tdTomato* Cre-reporter allele with chromosome (Chr.), exons (Ex) and poly-adenylation sites (pA). **D.** Expression of tdTomato of *Notch2-CreER^{T2-SAT}* animals with GFAP, PCNA or Dcx with split channels of Figure 1E-F. Arrows

point to tdTomato marker double-positive cells. **E.** Quantification of coexpression of GFAP, PCNA or Dcx with tdTomato. **F.** Schemes of floxed *Notch1*, *Notch2* and *Rbpj* loci, *Hes5::CreER^{T2}* transgene and *Rosa26R::GFP* Cre-reporter allele with chromosome (Chr.), exons, LoxP, and poly-adenylation sites (pA). **G.** Schematic representation of tamoxifen administration regiment and analysis of low-dose recombination and lineage analysis for driver in immunofluorescent costainings of GFP⁺ cells with GFAP, PCNA and Dcx. Values are means \pm SD; Control (C57BL/6J) animals n = 4, *Notch2-CreER^{T2-SAT}* animals n = 3; Low-dose analysis n = 3. Scale bars = 15 μ m in **A** (GFAP and Dcx) and **D** (GFAP and Dcx), 10 μ m in **A** (PCNA), **D** (PCNA) and **G**.

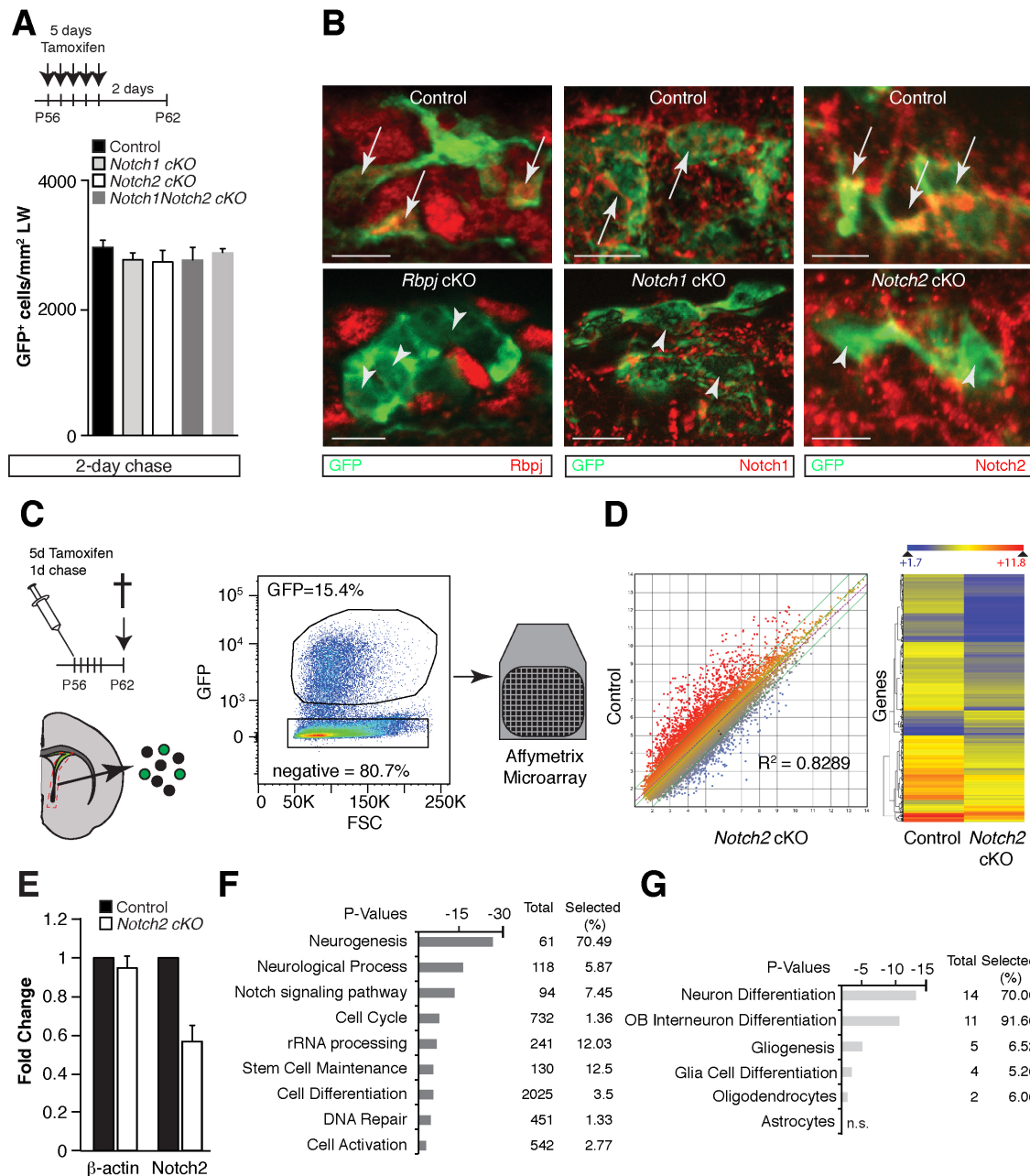


Figure S2. Acute loss of Notch signaling results in activation of quiescent NSCs. Related to Figure 2, Table S2 and Table S3.

A. Schematic representation of tamoxifen administration regiment, analyzed genotypes and levels of recombined GFP⁺ cells 2 days after tamoxifen administration. **B.** Recombination efficiency in Control and (from left to right) *Rbpj* cKO, *Notch1* cKO and *Notch2* cKO animals. Arrows point toward GFP⁺ marker⁺ cells, arrowheads towards GFP⁺, *Notch1* or *Notch2* ablated cells, respectively. **C.** Scheme of experimental setup. Following 5 days of tamoxifen induced mice were sacrificed 1-day later and *Hes5::CreER^{T2}*-derived (GFP⁺). Control or *Notch2* cKO V-SVZ cells were isolated by FACS and RNA prepared for microarray analysis. **D.** Scatter plot of mean Control versus *Notch2* cKO gene expression (log2). **E.** Confirmation of *Notch2* depletion in sorted cells **F.** Gene ontology (GO) analysis of differentially-expressed genes in *Notch2* cKO versus Control with significance, total genes in category and percent differentially expressed. **G.** GO analysis and top targets within Neurogenesis

category in *Notch2* cKO versus Control with significance, total genes in category and percent differentially expressed. Values are means \pm SD. 2-day chase: Control n = 5, *Notch1* cKO n = 6, *Notch2* cKO n = 5, *Notch1Notch2* cKO n = 4, *Rbpj* cKO n = 4. Scale bars = 10 μ m in **B**.

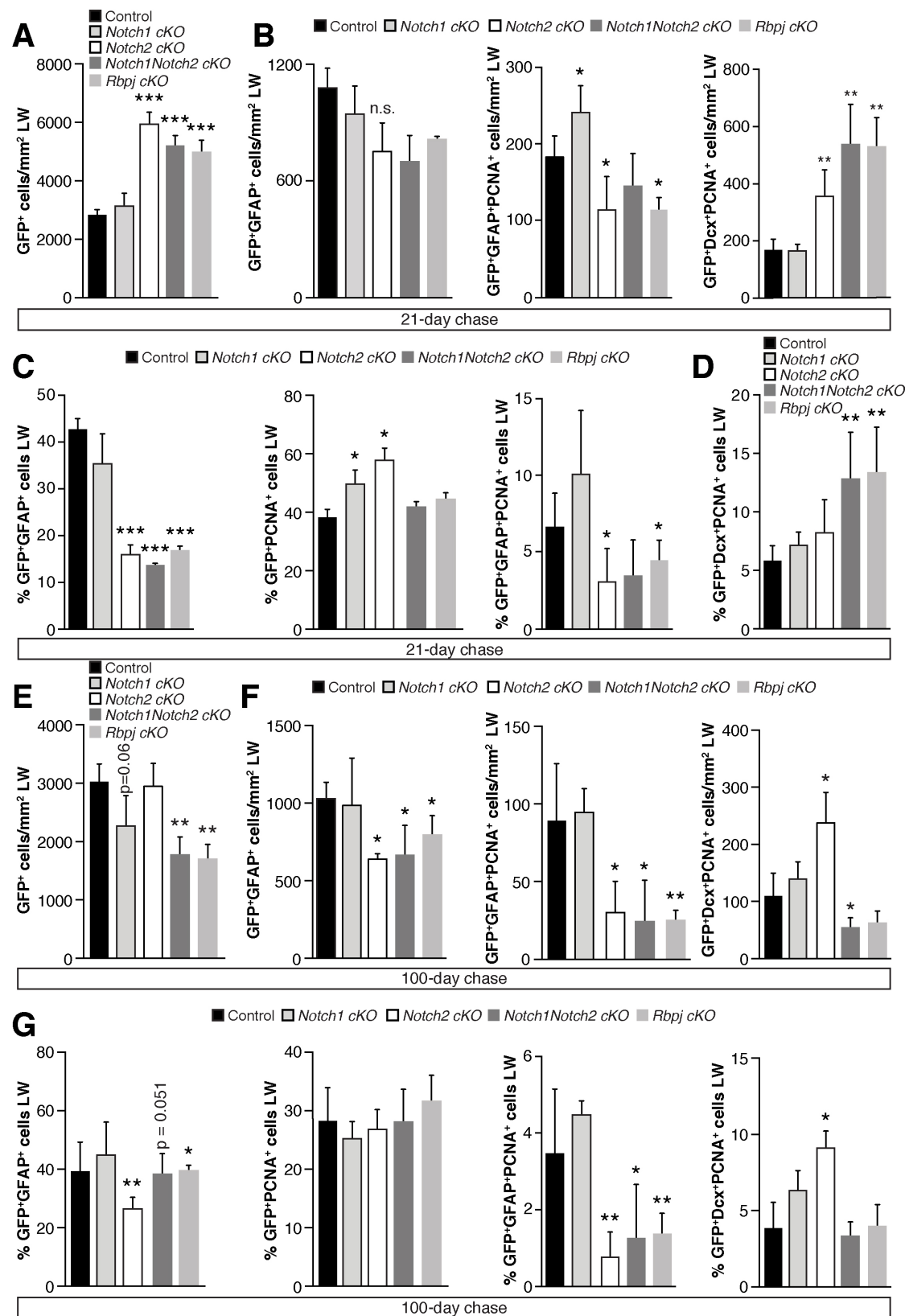


Figure S3. Notch1 and Notch2 have distinct functions in adult neurogenesis. Related to Figure 3 and Table S4.

A. Quantification and analysis of total *Hes5::CreER*^{T2}-derived (GFP⁺) cells. **B.** GFP⁺GFAP⁺ NSCs and GFP⁺GFAP⁺PCNA⁺ proliferating NSCs. **C.** Percentage of GFP⁺GFAP⁺ NSCs, GFP⁺PCNA⁺ proliferating cells and GFP⁺GFAP⁺PCNA⁺ proliferating NSCs. **D.** Percentage of GFP⁺Dcx⁺PCNA⁺ proliferating neuroblasts in the

LW of the V-SVZ in Control, *Notch1* cKO, *Notch2* cKO, *Notch1Notch2* cKO and *Rbpj* cKO mice 21 days post-tamoxifen induction. **E.** Quantification of the total number of *Hes5::CreER^{T2}*-derived (GFP⁺) cells. **F.** GFP⁺GFAP⁺ NSCs and GFP⁺GFAP⁺PCNA⁺ proliferating NSCs and **G.** Percentage of GFP⁺GFAP⁺ NSCs, GFP⁺PCNA⁺ proliferating cells and GFP⁺GFAP⁺PCNA⁺ proliferating NSCs in the V-SVZ of Control, *Notch2* cKO, *Notch1Notch2* cKO and *Rbpj* cKO mice 100 days post-tamoxifen induction. Values are means \pm SD; * - $p < 0.05$, ** - $p < 0.01$, *** - $p < 0.001$, 21-day chase: Control $n = 6$, *Notch1* cKO $n = 4$, *Notch2* cKO $n = 5$, *Notch1Notch2* cKO $n = 6$, *Rbpj* cKO $n = 4$, 100-day chase: Control $n = 5$, *Notch1* cKO $n = 4$, *Notch2* cKO $n = 4$, *Notch1Notch2* cKO $n = 4$, *Rbpj* cKO $n = 4$.

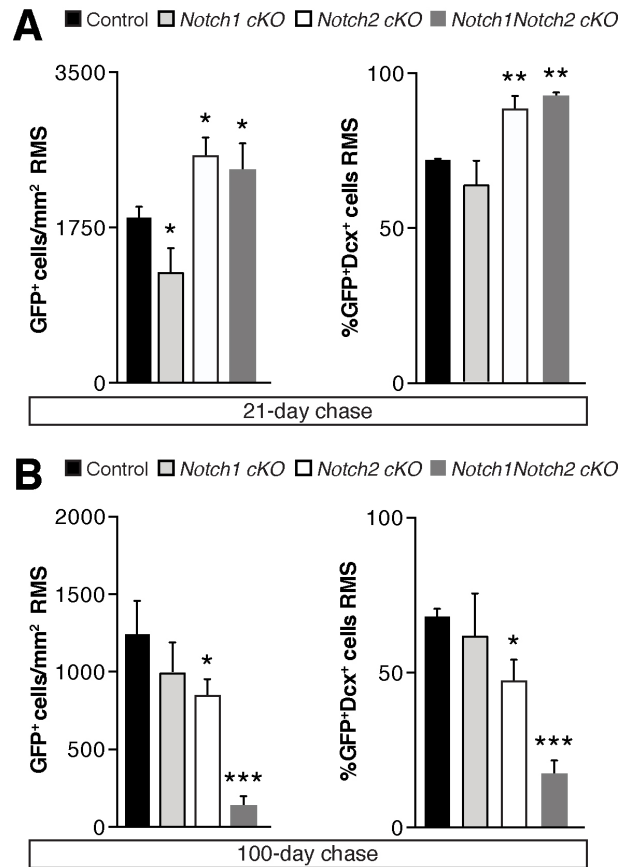


Figure S4. NSC activation projects down the rostral migratory stream. Related to Figure 4 and Table S5.

A. Quantification and analysis of the total GFP⁺ progeny and the percentage GFP⁺Dcx⁺ in the RMS of Control, *Notch1* cKO, *Notch2* cKO and *Notch1Notch2* cKO mice 21 days post-tamoxifen induction. **B.** Quantification and analysis of the total GFP⁺ progeny and the percentage GFP⁺Dcx⁺ in the RMS of Control, *Notch1* cKO, *Notch2* cKO and *Notch1Notch2* cKO mice 100 days post-tamoxifen induction. Values are means \pm SD; * - $p < 0.05$, ** - $p < 0.01$, *** - $p < 0.001$, 21-day chase: Control $n = 6$, *Notch1* cKO $n = 4$, *Notch2* cKO $n = 5$, *Notch1Notch2* cKO $n = 6$, 100-day chase: Control $n = 5$, *Notch1* cKO $n = 4$, *Notch2* cKO $n = 4$, *Notch1Notch2* cKO $n = 4$.

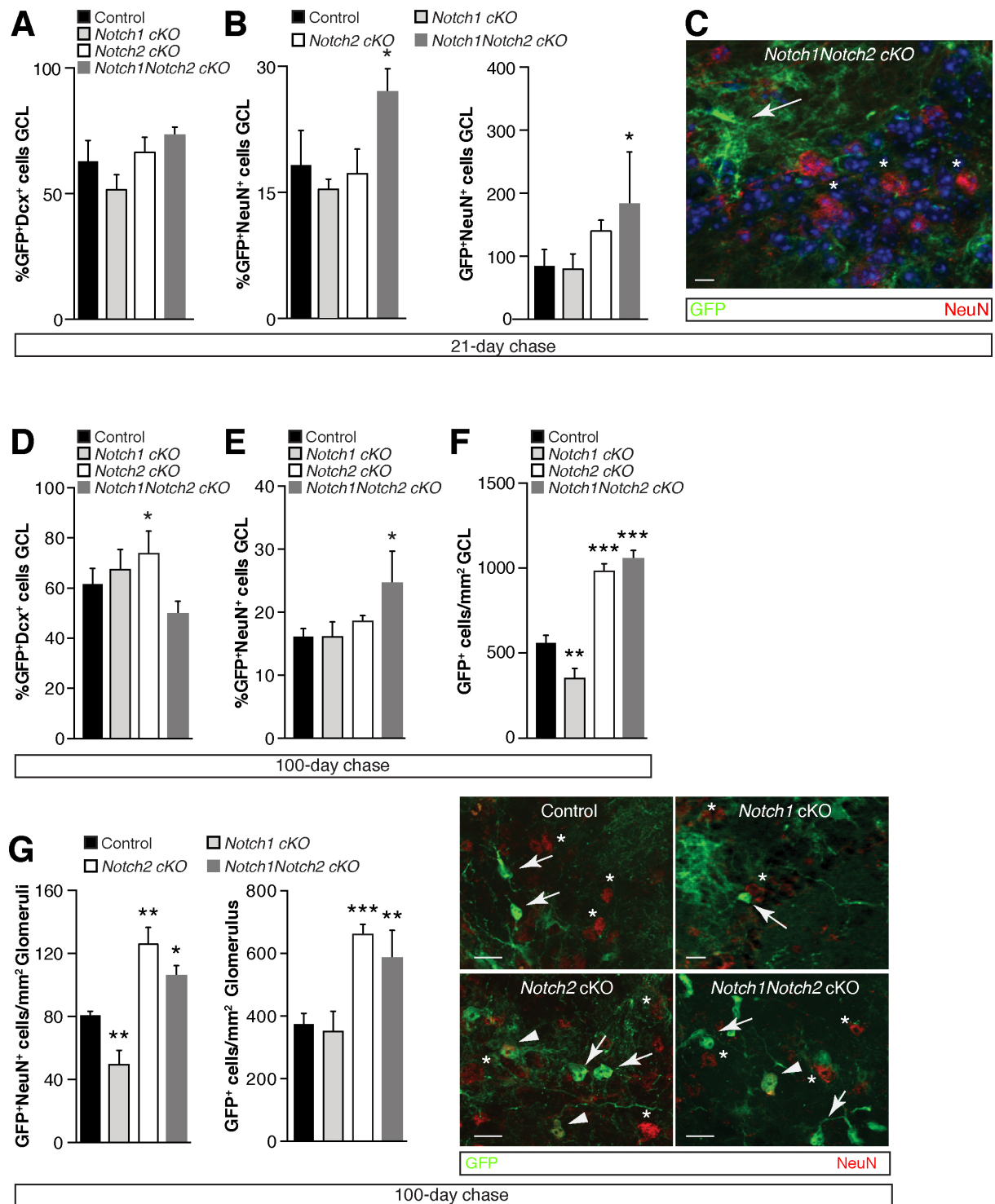


Figure S5. Notch signal manipulation affects the lineage into the OB. Related to Figure 5 and Table S6.

A. Percentage of GFP⁺Dcx⁺ neuroblasts in the GCL 21 days after tamoxifen administration in Control, *Notch1* cKO, *Notch2* cKO and *Notch1Notch2* cKO. **B.** GFP⁺NeuN⁺ cells in the GCL 21 days after tamoxifen administration in Control, *Notch1* cKO, *Notch2* cKO and *Notch1Notch2* cKO. **C.** At 21 days after tamoxifen administration, no new neurons have integrated into the glomeruli of the OB. Arrows point to GFP⁺ cells, asterisk mark NeuN⁺ cells. **D.** Percentage of GFP⁺Dcx⁺ neuroblasts in the GCL 100 days after tamoxifen administration in Control, *Notch1* cKO, *Notch2* cKO and *Notch1Notch2* cKO. **E.** Percentage of GFP⁺NeuN⁺ neurons in the GCL 100 days after tamoxifen administration in Control, *Notch1* cKO, *Notch2* cKO and *Notch1Notch2* cKO. **F.** Total number of recombined GFP⁺ cells in the GCL 100 days after tamoxifen administration in Control, *Notch1* cKO, *Notch2* cKO and *Notch1Notch2* cKO. **G.** Total number of GFP⁺NeuN⁺ neurons and recombined GFP⁺ cells in the glomeruli 100 days after tamoxifen administration in Control, *Notch1* cKO, *Notch2* cKO and *Notch1Notch2* cKO. Arrows point to GFP⁺ cells, asterisk mark NeuN⁺ cells, arrowheads point to GFP⁺NeuN⁺ cells. Values are means \pm SD; * - $p < 0.05$, ** - $p < 0.01$, *** - $p < 0.001$, 21-day chase:

Control n = 6, *Notch1* cKO n = 4, *Notch2* cKO n = 5, *Notch1Notch2* cKO n = 6, 100-day chase: Control n = 5, *Notch1* cKO n = 4, *Notch2* cKO n = 4, *Notch1Notch2* cKO n = 4, Scale bars = 15 μ m in C and G.

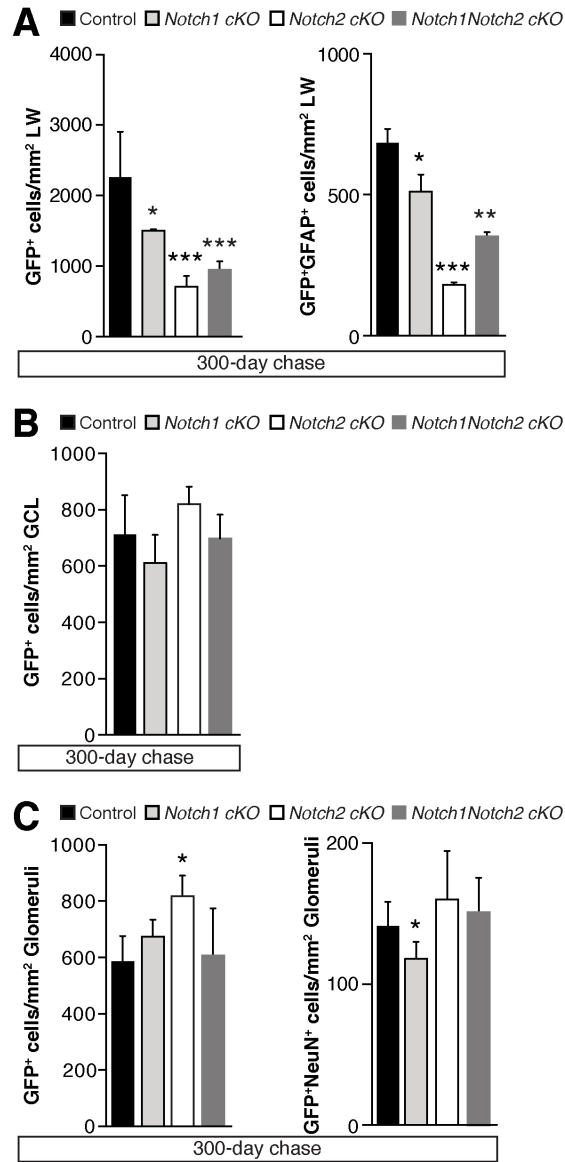


Figure S6. Notch signal manipulation affects the lineage into the OB. Related to Figure 6 and Table S7.

A. Quantification of total number of GFP⁺ cells and GFP⁺GFAP⁺ cells in the LW of the V-SVZ in Control, *Notch1* cKO, *Notch2* cKO and *Notch1Notch2* cKO mice 300 days after tamoxifen administration. **B.** Quantification of total number of GFP⁺ cells in the GCL 300 days after tamoxifen administration. **C.** Quantification of total number of GFP⁺ cells and GFP⁺NeuN⁺ neurons in the glomeruli in Control, *Notch1* cKO, *Notch2* cKO and *Notch1Notch2* cKO mice 300 days after tamoxifen administration. Values are means \pm SD; * - $p < 0.05$, ** - $p < 0.01$, *** - $p < 0.001$, 300-day chase: Control n = 4, *Notch1* cKO n = 3, *Notch2* cKO n = 3, *Notch1Notch2* cKO n = 3.

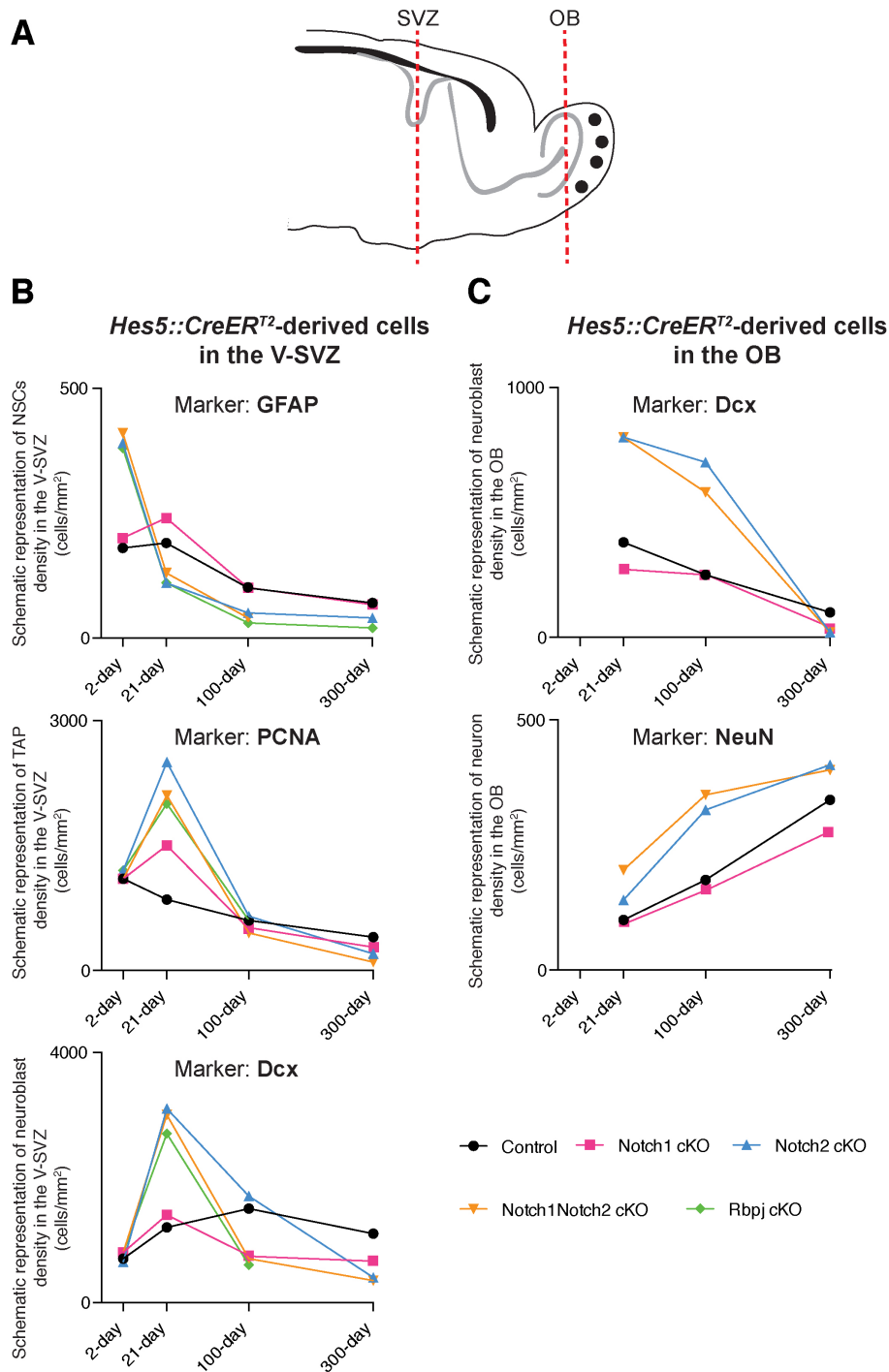


Figure S7. Notch ablation affects the neurogenic lineage. Related to Figure 7.

A. Scheme of a sagittal section of the adult mouse brain showing the plane of section and regions of analysis in the SVZ and OB. **B.** Summary of the changes in cell-type specific marker expression in the V-SVZ in *Notch1* cKO, *Notch2* cKO, *Notch1Notch2* cKO and *Rbpj* cKO animals over time compared to Control animals. **C.** Summary of the changes in cell-type specific marker expression in the OB in *Notch1* cKO, *Notch2* cKO and *Notch1Notch2* cKO animals over time compared to Control animals.

SUPPLEMENTAL DATA

Table S1, related to Figure 1 and Figure S1.

Table for the coexpression data of Notch signaling components with lineage markers. Coexpression of lineage markers with Rbpj or coexpression of lineage marker with tdTomato of *Notch2-CreER^{T2-SAT}* lineage tracing in percent per lineage marker in the lateral wall V-SVZ.

	GFAP	PCNA	Dcx
Rbpj	n.d.	100.0 ± 0.0	100.0 ± 0.0
tdTomato	93.8 ± 5.9	93.8 ± 2.8	42.4 ± 12.7

Table S2, related to Figure 2 and Figure S2.

Tables showing the number of GFP⁺ cells per mm². **A.** Knockout efficiency in recombined, GFP⁺ cells in percentage. **B.** GFP⁺ cells (per mm²) 2 days after tamoxifen administration in Control, *Notch1* cKO, *Notch2* cKO, *Notch1Notch2* cKO and *Rbpj* cKO in the lateral wall V-SVZ. **C.** Expression of lineage markers by recombined GFP⁺ cells in Control, *Notch1* cKO, *Notch2* cKO, *Notch1Notch2* cKO and *Rbpj* cKO in the V-SVZ.

A. Knockout efficiency

	Percentage GFP ⁺ cells	
	Control	Knockout
Notch1 ⁺	75.2 ± 8.2	19.1 ± 11.2
p-value (t-test)		0.0035 (**)
Notch2 ⁺	81.3 ± 9.7	18.9 ± 12.1
p-value (t-test)		0.0026 (**)
Rbpj ⁺	88.8 ± 8.4	13.8 ± 4.7
p-value (t-test)		< 0.0001 (***)

B. GFP⁺ cells 2 days post-tamoxifen administration

GFP ⁺ cells (mm ²)	Control	<i>Notch1</i> cKO	<i>Notch2</i> cKO	<i>Notch1Notch2</i> cKO	<i>Rbpj</i> cKO
2 days	2949.3 ± 125.8	2760.1 ± 112.0	2712.9 ± 197.9	2754.8 ± 201.2	2845.5 ± 79.2

C. GFP⁺ cells costained with specific markers, 2 days after tamoxifen administration

5-day TAM + 2 days chase	GFP+GFAP ⁺ (mm ²)	GFP+GFAP+PCNA ⁺ (mm ²)	GFP+PCNA ⁺ (mm ²)	GFP+Dcx ⁺ (mm ²)
Control	1326.4 ± 157.2	185.3 ± 85.3	1131.0 ± 102.0	713.6 ± 13.7
<i>Notch1</i> cKO	1127.4 ± 43.7	223.6 ± 23.7	1096.7 ± 56.2	880.3 ± 112.9
p-value (t-test)	0.135 (n.s.)	0.421 (n.s.)	0.662 (n.s.)	0.212 (n.s.)
<i>Notch2</i> cKO	903.3 ± 129.7	394.3 ± 28.3	1198.4 ± 294.8	690.3 ± 276.7
p-value (t-test)	0.217 (n.s.)	0.015 (*)	0.296 (n.s.)	0.831 (n.s.)
<i>Notch1Notch2</i> cKO	997.9 ± 24.7	444.2 ± 43.3	1093.7 ± 147.7	939.3 ± 87.2
p-value (t-test)	0.363 (n.s.)	0.046 (*)	0.541 (n.s.)	0.0414 (n.s.)
<i>Rbpj</i> cKO	998.2 ± 48.3	372.0 ± 41.5	1270.8 ± 95.7	937.2 ± 221.6
p-value (t-test)	0.125 (n.s.)	0.044 (*)	0.187 (n.s.)	0.037 (n.s.)

Table S3, related to Figure S2.

See Supplemental Excel table showing results of Microarray analysis of Control vs. *Notch2* cKO animals.

Table S4, related to Figure 3 and Figure S3.

Tables showing the number and marker expression of GFP⁺ cells per mm², 21 days and 100 days post-tamoxifen administration. **A.** GFP⁺ cells (per mm²) 21 and 100 days after tamoxifen administration in Control, *Notch1* cKO, *Notch2* cKO, *Notch1Notch2* cKO and *Rbpj* cKO in the V-SVZ. **B.** Expression of lineage markers by recombined GFP⁺ cells 21 days post-tamoxifen administration in Control, *Notch1* cKO, *Notch2* cKO, *Notch1Notch2* cKO and *Rbpj* cKO in the V-SVZ. **C.** Expression of lineage markers by recombined GFP⁺ cells 21 days post-tamoxifen administration in Control, *Notch1* cKO, *Notch2* cKO, *Notch1Notch2* cKO and *Rbpj* cKO in the V-SVZ.

A. GFP⁺ cells in the V-SVZ.

GFP ⁺ cells (mm ²)	Control	<i>Notch1</i> cKO	<i>Notch2</i> cKO	<i>Notch1Notch2</i> cKO	<i>Rbpj</i> cKO
21 days	2827.3 ± 191.2	3127.0 ± 450.3	5942.1 ± 414.3	5212.8 ± 345.9	4998.6 ± 395.7
100 days	3026.7 ± 303.8	2265.9 ± 460.7	2945.2 ± 391.5	1774.3 ± 302.7	1703.2 ± 250.1

B. GFP⁺ cells coexpressing lineage markers 21 days after tamoxifen administration.

5-day TAM + 21 days chase	GFP+GFAP ⁺ (mm ²)	GFP+GFAP+PCNA ⁺ (mm ²)	GFP+PCNA ⁺ (mm ²)	GFP+Dcx ⁺ (mm ²)	GFP+Dcx+PCNA ⁺ (mm ²)
Control	1156.5 ± 97.5	185.3 ± 27.3	730.2 ± 193.1	1341.8 ± 447.2	179.2 ± 20.4
<i>Notch1</i> cKO	964.9 ± 101.7	240.4 ± 40.8	1747.3 ± 410.0	1489.8 ± 635.8	174.7 ± 9.8
p-value (t-test)	0.627 (n.s.)	0.038 (*)	0.521 (n.s.)	0.240 (n.s.)	0.358 (n.s.)
<i>Notch2</i> cKO	798.7 ± 121.7	107.6 ± 80.1	2502.1 ± 705.5	3284.5 ± 342.3	374.8 ± 98.7
p-value (t-test)	0.186 (n.s.)	0.044 (*)	0.0032 (**)	<0.001 (***)	0.014 (**)
<i>Notch1Notch2</i> cKO	701.5 ± 132.8	152.1 ± 30.2	2155.7 ± 378.9	3008.5 ± 328.9	521.7 ± 116.2
p-value (t-test)	0.063 (n.s.)	0.056 (n.s.)	0.008 (**)	0.010 (**)	0.003 (**)
<i>Rbpj</i> cKO	842.3 ± 23.8	111.2 ± 12.6	1956.3 ± 13.2	2426.3 ± 147.4	513.6 ± 102.8
p-value (t-test)	0.055 (n.s.)	0.032 (*)	0.043 (*)	0.002 (**)	0.002 (**)

C. GFP⁺ cells coexpressing lineage markers 100 days after tamoxifen administration.

5-day TAM + 100 days chase	GFP+GFAP ⁺ (mm ²)	GFP+GFAP+PCNA ⁺ (mm ²)	GFP+PCNA ⁺ (mm ²)	GFP+Dcx ⁺ (mm ²)	GFP+Dcx+PCNA ⁺ (mm ²)
Control	1019.5 ± 75.5	85.5 ± 40.2	610.0 ± 127.4	1583.8 ± 573.3	105.8 ± 42.3
<i>Notch1</i> cKO	972.1 ± 199.2	91.2 ± 20.2	545.5 ± 94.0	648.8 ± 40.3	132.7 ± 29.6
p-value (t-test)	0.46 (n.s.)	0.52 (n.s.)	0.612 (n.s.)	0.009 (**)	0.217 (n.s.)
<i>Notch2</i> cKO	672.4 ± 24.6	30.2 ± 19.2	675.1 ± 120.4	1897.7 ± 327.9	240.2 ± 54.7
p-value (t-test)	0.048 (*)	0.021 (*)	0.126 (n.s.)	0.219 (n.s.)	0.015 (*)
<i>Notch1Notch2</i> cKO	685.9 ± 142.7	24.1 ± 28.8	463.6 ± 71.4	550.1 ± 73.4	48.7 ± 9.7
p-value (t-test)	0.04 (*)	0.018 (*)	0.44 (n.s.)	<0.001 (***)	0.048 (*)
<i>Rbpj</i> cKO	727.8 ± 92.5	25.1 ± 8.1	609.8 ± 167.5	461.7 ± 8.5	50.1 ± 12.2
p-value (t-test)	0.050 (*)	0.008 (**)	0.087 (n.s.)	<0.001 (***)	0.056 (n.s.)

Table S5, related to Figure 4 and Figure S4.

Tables showing the number and marker expression of GFP⁺ cells per mm² 21 days and 100 days post-tamoxifen administration and area of RMS. **A.** GFP⁺ cells (per mm²), marker expression and area 21 days after tamoxifen administration in Control, *Notch1* cKO, *Notch2* cKO, and *Notch1Notch2* cKO in the RMS. **B.** GFP⁺ cells (per mm²), marker expression and area 100 days after tamoxifen administration in Control, *Notch1* cKO, *Notch2* cKO, and *Notch1Notch2* cKO in the RMS.

A. GFP⁺ cells in the RMS, 21 days post-tamoxifen administration.

5-day TAM + 21 days chase	GFP⁺ (mm²)	GFP⁺Dcx⁺ (mm²)	Area RMS (mm²)
Control	1763.3 ± 52.1	1181.6 ± 47.2	0.21 ± 0.02
<i>Notch1</i> cKO	1150.6 ± 302.1	772.4 ± 227.9	0.18 ± 0.03
p-value (t-test)	0.025 (*)	0.030 (*)	0.11 (n.s.)
<i>Notch2</i> cKO	2602.0 ± 97.6	2204.3 ± 122.3	0.26 ± 0.04
p-value (t-test)	0.028 (*)	0.002 (**)	0.041 (*)
<i>Notch1Notch2</i> cKO	2498.1 ± 245.7	2198.5 ± 141.7	0.28 ± 0.05
p-value (t-test)	0.033 (*)	0.003 (**)	0.035 (*)

B. GFP⁺ cells in the RMS, 100 days post-tamoxifen administration.

5-day TAM + 100 days chase	GFP⁺ (mm²)	GFP⁺Dcx⁺ (mm²)	Area RMS (mm²)
Control	1230.3 ± 257.2	893.9 ± 135.1	0.18 ± 0.01
<i>Notch1</i> cKO	998.4 ± 205.5	625.5 ± 73.4	0.17 ± 0.03
p-value (t-test)	0.14 (n.s.)	0.019 (*)	0.30 (n.s.)
<i>Notch2</i> cKO	867.2 ± 103.7	524.3 ± 45.7	0.16 ± 0.02
p-value (t-test)	0.016 (*)	0.021 (*)	0.089 (n.s.)
<i>Notch1Notch2</i> cKO	98.3 ± 17.3	23.3 ± 7.3	0.11 ± 0.00
p-value (t-test)	<0.0001 (***)	<0.0001 (***)	0.0087 (**)

Table S6, related to Figure 5 and Figure S5.

Tables showing the number and marker expression of GFP⁺ cells per mm², 21 days and 100 days post-tamoxifen administration. GFP⁺ cells (per mm²) and marker expression **A.** 21 days after tamoxifen administration in Control, *Notch1* cKO, *Notch2* cKO, and *Notch1Notch2* cKO in the granule cell layer. **B.** GFP⁺ cells (per mm²) and marker expression 100 days after tamoxifen administration in Control, *Notch1* cKO, *Notch2* cKO, and *Notch1Notch2* cKO in the granule cell layer. **C.** GFP⁺ cells (per mm²) and marker expression 100 days after tamoxifen administration in Control, *Notch1* cKO, *Notch2* cKO, and *Notch1Notch2* cKO in the glomeruli.

A. GFP⁺ cells in the granule cell layer, 21 days after tamoxifen administration

5-day TAM + 21 days chase	GFP⁺Dcx⁺ (mm²)	GFP⁺NeuN⁺ (mm²)
Control	382.5 ± 38.7	85.3 ± 19.4
<i>Notch1</i> cKO	255.2 ± 33.3	80.8 ± 20.3
p-value (t-test)	0.045 (*)	0.38 (n.s.)
<i>Notch2</i> cKO	802.1 ± 103.7	135.8 ± 11.5
p-value (t-test)	<0.0001 (***)	0.141 (n.s.)
<i>Notch1Notch2</i> cKO	791.3 ± 98.6	168.5 ± 89.0
p-value (t-test)	<0.0001 (***)	0.019 (*)

B. GFP⁺ cells in the granule cell layer, 100 days after tamoxifen administration

5-day TAM + 100 days chase	GFP⁺ (mm²)	GFP+Dcx⁺ (mm²)	GFP+NeuN⁺ (mm²)
Control	511.2 ± 15.3	210.8 ± 173.8	85.7 ± 27.1
<i>Notch1</i> cKO	337.3 ± 30.8	231.7 ± 92.7	62.1 ± 24.9
p-value (t-test)	0.002 (**)	0.35 (n.s.)	0.16 (n.s.)
<i>Notch2</i> cKO	999.1 ± 11.2	714.9 ± 75.8	175.3 ± 41.3
p-value (t-test)	<0.0001 (***)	0.006 (**)	0.058 (n.s.)
<i>Notch1Notch2</i> cKO	1003.3 ± 75.2	575.7 ± 21.8	245.3 ± 91.2
p-value (t-test)	<0.0001 (***)	0.022 (*)	0.007 (**)

C. GFP⁺ cells in the glomeruli, 100 days after tamoxifen administration

5-day TAM + 100 days chase	GFP⁺ (mm²)	GFP+NeuN⁺ (mm²)
Control	384.5 ± 21.3	79.2 ± 11.1
<i>Notch1</i> cKO	378.6 ± 29.7	51.3 ± 9.6
p-value (t-test)	0.40 (n.s.)	0.015 (*)
<i>Notch2</i> cKO	660.6 ± 25.6	122.8 ± 15.3
p-value (t-test)	<0.0001 (***)	0.002 (**)
<i>Notch1Notch2</i> cKO	585.8 ± 64.2	105.3 ± 7.7
p-value (t-test)	0.005 (**)	0.021 (*)

Table S7, related to Figure 6 and Figure S6.

Tables showing the number and marker expression of GFP⁺ cells per mm², 300 days post-tamoxifen administration. **A.** GFP⁺ cells (per mm²) 300 days after tamoxifen administration in Control, *Notch1* cKO, *Notch2* cKO, and *Notch1Notch2* cKO in the V-SVZ. **B.** GFP⁺ cells (per mm²) and marker expression 300 days after tamoxifen administration in Control, *Notch1* cKO, *Notch2* cKO, and *Notch1Notch2* cKO in the V-SVZ. **C.** GFP⁺ cells (per mm²) and marker expression 300 days after tamoxifen administration in Control, *Notch1* cKO, *Notch2* cKO, and *Notch1Notch2* cKO in the granule cell layer of the OB. **D.** GFP⁺ cells (per mm²) and marker expression 300 days after tamoxifen administration in Control, *Notch1* cKO, *Notch2* cKO, and *Notch1Notch2* cKO in the glomeruli of the OB.

A. GFP⁺ cells in the V-SVZ

GFP⁺ cells (mm²)	Control	<i>Notch1</i> cKO	<i>Notch2</i> cKO	<i>Notch1Notch2</i> cKO
300 days	2166.7 ± 565.6	1427.3 ± 8.4	710.1 ± 101.7	948.6 ± 71.2

B. GFP⁺ cells in the V-SVZ

5-day TAM + 300 days chase	GFP+GFAP⁺ (mm²)	GFP+PCNA⁺ (mm²)	GFP+Dcx⁺ (mm²)
Control	687.6 ± 20.2	667.1 ± 128.0	1342.3 ± 112.8
<i>Notch1</i> cKO	512.3 ± 35.5	307.1 ± 95.4	623.3 ± 11.8
p-value (t-test)	0.049 (*)	0.022 (*)	0.034 (*)
<i>Notch2</i> cKO	181.6 ± 7.9	209.1 ± 14.5	340.8 ± 62.8
p-value (t-test)	<0.001 (***)	0.006 (**)	<0.001 (***)
<i>Notch1Notch2</i> cKO	352.1 ± 7.2	93.7 ± 2.7	281.7 ± 42.7
p-value (t-test)	0.004 (**)	<0.001 (***)	<0.001 (***)

C. GFP⁺ cells in the GCL of the OB

5-day TAM + 300 days chase	GFP⁺ (mm²)	GFP⁺Dcx⁺ (mm²)	GFP⁺NeuN⁺ (mm²)
Control	707.6 ± 110.8	61.5 ± 39.9	222.3 ± 13.1
<i>Notch1</i> cKO	595.6 ± 107.3	12.3 ± 8.9	183.8 ± 21.3
p-value (t-test)	0.11 (n.s.)	0.047 (*)	0.026 (*)
<i>Notch2</i> cKO	801.6 ± 45.9	11.1 ± 3.1	266.8 ± 61.2
p-value (t-test)	0.534 (n.s.)	0.007 (**)	0.241 (n.s.)
<i>Notch1Notch2</i> cKO	706.1 ± 74.2	14.7 ± 2.9	294.3 ± 39.0
p-value (t-test)	0.431 (n.s.)	0.008 (**)	0.157 (n.s.)

D. GFP⁺ cells in the glomeruli of the OB

5-day TAM + 300 days chase	GFP⁺ (mm²)	GFP⁺NeuN⁺ (mm²)
Control	591.3 ± 98.9	146.6 ± 14.4
<i>Notch1</i> cKO	680.0 ± 21.6	120.5 ± 13.7
p-value (t-test)	0.09 (n.s.)	0.039 (*)
<i>Notch2</i> cKO	800.2 ± 84.2	173.3 ± 26.2
p-value (t-test)	0.042 (*)	0.196 (n.s.)
<i>Notch1Notch2</i> cKO	602.1 ± 193.4	157.6 ± 20.0
p-value (t-test)	0.08 (n.s.)	0.295 (n.s.)

SUPPLEMENTAL EXPERIMENTAL PROCEDURES

Animals and husbandry according to ARRIVE-guidelines

Hes5::GFP, *Hes5::CreER^{T2}*, *Notch2::CreER^{T2-SAT}*, *Rosa26R::GFP*, *Rosa26R::tdTomato*, floxed *Notch1*, floxed *Notch2*, floxed *Rbpj* mice have been described elsewhere (Basak and Taylor, 2007; Besseyrias et al., 2007; Schouwey et al., 2007; Fre et al., 2011; Basak et al., 2012; Lugert et al., 2012). Mice were maintained on a C57Bl6 genetic background and kept on a 12-hour day/night cycle with food (Kliba Nafag Haltungsextrudat 3436) and water (filtered and autoclaved) *ad libitum* under specified pathogen free conditions and according to Swiss Federal and Swiss Veterinary office regulations under license numbers 2537 and 2538 (Ethics commission Basel-Stadt, Basel Switzerland). Animals were housed in IVC Greenline Techniplast GM500 cages on Aspen bedding (Tapvei). 5-6 animals were cohoused per cage at an ambient temperature of $22 \pm 2^\circ\text{C}$ and $55 \pm 15\%$ humidity. Animals for experiments were selected at random based on genotype. Experimental animals were virgins and all experiments were performed with a mix of genders (43 females, 37 males in total). Animals were genotyped after endpoint analysis.

Administration of tamoxifen and tissue preparation for immunochemical staining

Adult mice 8-10 weeks of age, weighing 20-30 grams, were used in the experiments. *Hes5::CreER^{T2}* mice carrying floxed *Rbpj*, floxed *Notch1* or floxed *Notch2* alleles were injected daily intraperitoneal (i.p.) for optimal recombination with 2 mg tamoxifen in corn oil (100 μl of 20 mg/ml) for five consecutive days, and thereafter housed in home cage and killed 2, 21, 100 or 300 days after the end of the treatment. Conditional gene knockout mutants were necessary as loss of *Rbpj* or *Notch* receptors is embryonic lethal. Conditional deletion allowed for mosaic analysis of gene function. Animals were injected intraperitoneal (i.p.) with a lethal dose of Ketamine-Xylazine and perfused with cold phosphate buffered saline (PBS) followed by 4% PFA in PBS. Brains were excised, fixed overnight in 4% PFA in PBS, cryoprotected with 30% sucrose in PBS at 4°C 48 hours, embedded and frozen in OCT (TissueTEK), and 30 μm floating sections cut by cryostat (Leica).

Ex vivo microarray analysis of tamoxifen-induced, recombined cells

Adult mice 8-10 weeks of age were used in the experiments. *Hes5::CreER^{T2}* mice carrying floxed *Notch2* alleles were injected daily intraperitoneal (i.p.) with 2 mg tamoxifen as stated previously. After five days consecutive administration, animals were sacrificed 24 hours after the end of the treatment. Animals were euthanized in CO_2 , brains were dissected in L15 Medium (GIBCO) and cut into 0.55 mm thick sections using a McIlwain tissue chopper. The SVZ was microdissected under a binocular microscope avoiding contamination from the striatum, and digested using a Papain solution and mechanical dissociation as described previously (Lugert et al., 2010). Cells were resuspended in Leibovitz medium (Life Technologies), filtered through a 40 μm cell strainer (Miltenyi Biotec) and sorted on a BD FACS Aria III. Cells were discriminated by forward and side-scatter (for live cells – from the control animals) and gated for GFP^- (wild-type levels) or GFP^+ populations. Cells were directly sorted into cooled Trizol (Life Technologies). Appropriate amount of Chloroform was added and RNA extraction was performed using Isopropanol with LiCl (0.75M). RNA was immediately frozen to -80°C . RNA quality was tested on a Fragment Analyzer (Advanced Analytical) using a high sensitivity RNA analysis kit (DNF-472). Samples were sent for Expression Profiling with Atlas Biolabs. Samples were subjected to a second quality control on an Agilent 2100 Bioanalyzer, small samples were amplified using the Ovation Picokit (NuGen) and then run on an Affymetric Biochip. GO analysis was done using Lasergene Arraystar (DNASar) software.

Quantitative PCR confirmation of *Notch2* knockout

Ex vivo mRNA was prepared as described above. Isolated RNA was treated with DNaseI (Roche). cDNA was prepared using BioScript (Bioline) and random hexamer primers. qPCR was performed using SensiMix SYBR kit (Bioline). Primers for PCR reactions are as follows:

GAPDH	Fwd: CTCCCACTCTTCCACCTTCG Rev: CCACCACCTGTTGCTGTAG
β -Actin	Fwd: AGGTGACAGCATTGCTTCTG Rev: GGGAGACCAAAGCCTTCATA
<i>Notch2</i> (Exon 26/27)	Fwd: CAGGAGGTGATAGGCTCTAAG Rev: GAAGCACTGGTCTGAATCTTG

Immunofluorescence staining of floating sections and antibodies

Immunostainings on sections was performed as described previously (Giachino and Taylor, 2009; Lugert et al., 2010). Briefly, sections were blocked at room temperature for 30 minutes with 10% normal donkey serum (Jackson ImmunoResearch) in PBS containing 0.5% TritonX-100. Primary antibodies diluted in 2.5% donkey serum blocking solution were incubated overnight. Sections were washed with PBS and incubated at room temperature for 1-2 hours with the corresponding secondary antibodies in 5% donkey serum blocking solution

and counter-stained with DAPI (1 µg/ml). Sections were mounted on glass slides (SuperFrost, Menzel) in DABCO mounting media and visualized using a Zeiss Observer with Apotome (Zeiss). For PCNA detection, the antigen was recovered at 80°C for 20 minutes in Sodium Citrate (10 mM, pH7.4).

Primary antibodies used were as follows: Anti-Doublecortin (goat, 1:500, Santa Cruz, sc-8066), anti-dsRed (rabbit, 1:500, CloneTech Takara, 632496), anti-Glial fibrillary acidic protein (mouse, 1:500, Sigma, G3893), anti-Glial fibrillary acidic protein (rabbit, 1:1000, Sigma, G9269), anti-GFP (chicken, 1:250, AvesLab, GFP-1020), anti-GFP (rabbit, 1:500, Invitrogen, A11122), anti-GFP, (sheep, 1:250, AbD Serotec, 4745-1051), anti-Neuronal nuclear antigen (mouse, 1:800, Millipore, MAB377), anti-Notch1 (rabbit, 1:100, (Nyfeler et al., 2005)), anti-Notch2 (rat, H. Robson Lausanne, 1:200), anti-Proliferating cell nuclear antigen (mouse 1:1000, DAKO, M0879), and anti-Rbpj (rabbit, 1:1000, Cell Signaling, 5313).

Secondary antibodies used were as follows: Donkey anti-rabbit Ig Cy3 conjugated (1:500, Jackson ImmunoResearch, 711165152), donkey anti-mouse Ig Cy3 conjugated (1:500, Jackson ImmunoResearch, 715165151), donkey anti-rabbit Ig Cy5 conjugated (1:300, Jackson ImmunoResearch, 711496152), donkey anti-mouse Ig Cy5 conjugated (1:300, Jackson ImmunoResearch, 715175151), donkey anti-rabbit Ig 488 conjugated (1:500, Jackson ImmunoResearch, 711545152), donkey anti-sheep Ig 488 conjugated (1:500, Jackson ImmunoResearch, 713095147), donkey anti-goat Ig Cy3 conjugated (1:500, Jackson ImmunoResearch, 705165147), and donkey anti-rat Ig Cy3 conjugated (1:500, Jackson ImmunoResearch, 712160153).

Quantification and statistical analysis

Stained sections were analyzed with a Zeiss Observer with Apotome (Zeiss). Images were processed with Photoshop or ImageJ. Data are presented as averages of a minimum of three sections per region and multiple animals (n in figure legends). Statistical significance was determined by two-tailed Student's t-test on mean values per animal, percentages were transformed into their arcsin value. Significance was determined at * - $p < 0.05$, ** - $p < 0.01$, *** - $p < 0.001$ or P-values are given in the graphs. Deviance from mean is displayed as standard deviation if not otherwise indicated. Complete data tables are provided in supplemental data and information.